GEOLOGIC NOTE

Impact of differential tectonic subsidence on isolated carbonate-platform evolution: Triassic of the Nanpanjiang Basin, south China

Daniel J. Lehrmann, Pei Donghong, Paul Enos, Marcello Minzoni, Brooks B. Ellwood, Michael J. Orchard, Zhang Jiyan, Wei Jiayong, Pete Dillett, Jon Koenig, Kelley Steffen, Dominic Druke, Jordayna Druke, Benjamin Kessel, and Trent Newkirk

ABSTRACT

The Nanpanjiang Basin of south China contains four exceptionally well-exposed, isolated Triassic carbonate platforms. Detailed mapping of two-dimensional transects and description of stratigraphic sections allow the reconstruction of facies architecture, sequence stratigraphy, and evolution of the platforms. Biostratigraphy, magnetic-susceptibility profiles, and volcanic-ash horizons allow chronostratigraphic correlation and, thus, a basinwide evaluation of mechanisms controlling platform evolution.

A comparison of platform architecture demonstrates that southerly platforms have substantially greater thickness, backstepping geometry, pinnacle development, and earlier drowning that resulted from greater tectonic subsidence proximal to a probable convergent margin along the southern perimeter of the basin. Felsic volcanics thicken southward and contributed to the termination of the southernmost platform, indicating the development of a volcanic arc along the southern margin of the South China tectonic block. The northernmost isolated platform had greater longevity and lesser accumulation and lacks backstepping and pinnacle phases of development. Basin-margin intertonguing relationships, or lack thereof, demonstrate that earlier siliciclastic influx into the basin to the south and concurrent starved-basin conditions to the north impacted the evolution of platform-margin geometries.

Manuscript received June 5, 2006; provisional acceptance August 24, 2006; revised manuscript received October 2, 2006; final acceptance October 16, 2006.
DOI:10.1306/10160606065

AUTHORS

Daniel J. Lehrmann ~ *Department of Geology, University of Wisconsin–Oshkosh, 800 Algoma Boulevard, Oshkosh, Wisconsin 54901; Lehrmann@uwosh.edu*

Daniel Lehrmann received his bachelor's degree from the University of Wisconsin–Oshkosh, his M.S. degree from the University of Wisconsin–Madison, and his Ph.D. from the University of Kansas. He worked as a research geologist for Exxon Production Research from 1993 to 1996. Since 1996, he has been a faculty member at the University of Wisconsin–Oshkosh.

Pei Donghong ~ *Department of Geology, University of Kansas, Lawrence, Kansas 66045; present address: University of Nevada–Reno, Reno, Nevada 89557*

Pei Donghong received his bachelor's degree from the Xinjiang Petroleum Institute and his M.S. degree from the Research Institute of Petroleum Exploration and Development, China National Petroleum Corporation. He conducted research for this project during his graduate studies at the University of Kansas. He is currently a graduate student in geophysics at the University of Nevada–Reno.

Paul Enos ~ *Department of Geology, University of Kansas, Lawrence, Kansas 66045*

Paul Enos is Emeritus Distinguished Professor at the University of Kansas, where he taught from 1982 to 2003 and where he received a B.S. degree in geology in 1956. He earned an M.S. degree at Stanford University and his Ph.D. from Yale University. From 1964 to 1970, he was a research geologist at Shell Development Company and was a faculty member at the State University of New York Binghamton from 1970 to 1982.

Marcello Minzoni ~ *Department of Geology, University of Kansas, Lawrence, Kansas 66045*

Marcello Minzoni received his B.S. and M.S. degrees from the University of Ferrara in Italy. He is currently completing his Ph.D. at the University of Kansas. Starting January 2007, he will be working for Shell International Exploration and Production Company. His interests are focused on the influence of tectonics on carbonate-platform evolution and termination.

Brooks B. Ellwood ~ *Louisiana State University, Baton Rouge, Louisiana 70803*

Brooks B. Ellwood received his bachelor's degree from Florida State University and his M.S. degree and his Ph.D. from the University of Rhode Island Graduate School of Oceanography. He did postdoctoral research at Ohio State University and was a faculty member at the University of Georgia and the University of Texas at Arlington, where he was acting chair. In 1999, he took the chair's position at Louisiana State University and is currently a faculty member there.

Michael J. Orchard ~ *Geological Survey of Canada, Vancouver, British Columbia, Canada, V6B 5J3*

Michael J. Orchard received his B.Sc. degree and his Ph.D. from the University of Hull in England and subsequently undertook postdoctoral research at Cambridge before joining the Geological Survey of Canada in 1979.

Zhang Jiyan ~ *Geological Survey of Guangxi, Guilin, Guangxi, People's Republic of China*

Zhang Jiyan is a senior geologist, recently retired from the Guangxi Geological Survey. He received his bachelor's degree from the Chengdu College of Geology. His interests are sedimentary geology and regional geology.

Wei Jiayong ~ *Guizhou Bureau of Geology, Guiyang, Guizhou, People's Republic of China*

Wei Jiayong is a senior geologist, recently retired from the Guizhou Bureau of Geology, where he had served since 1957. He received his bachelor's degree from China College of Geology, Beijing. His interests are sedimentary geology, paleontology, and regional geology.

Pete Dillett ~ *Department of Geology, University of Wisconsin–Oshkosh, Oshkosh, Wisconsin 54901; present address: Chevron North America Exploration and Production, McKittrick, California 93251*

Pete Dillett received his bachelor's degree from the University of Wisconsin–Oshkosh and his M.S. degree from the University of Kansas. He joined Chevron North America Exploration and Production in 2004, where he works as an earth scientist in California. His interests are carbonate sequence stratigraphy and reservoir-monitoring technologies.

Jon Koenig ~ *Department of Geology, University of Wisconsin–Oshkosh, Oshkosh, Wisconsin 54901; present address: Anadarko Petroleum Corporation, Houston, Texas 77251*

Jon Koenig received his bachelor's degree from the University of Wisconsin–Oshkosh and his M.S. degree from Baylor University. He joined Anadarko Petroleum Company in 2005, where he works as a development geologist. His interests are carbonate sedimentology and facies models.

Kelley Steffen ~ *Department of Geology, University of Wisconsin–Oshkosh, Oshkosh, Wisconsin 54901; present address: ExxonMobil Upstream Research Company, Houston, Texas 77252*

Kelley Steffen received her bachelor's degree from the University of Wisconsin–Oshkosh and her M.S. degree from the University of Miami, Rosenstiel School of Marine and Atmospheric Sciences. She has been a research geologist for ExxonMobil Upstream Research since 2005. Her interests are carbonate sedimentology and modern processes.

Dominic Druke ~ *Department of Geology, University of Wisconsin–Oshkosh, Oshkosh, Wisconsin 54901; present address: Shell Exploration and Production Company, Houston, Texas 77079*

Dominic Druke received his bachelor's degree from the University of Wisconsin–Oshkosh and his M.S. degree

Comparative analysis of platform evolution shows that the timing and rates of tectonic subsidence controlled the timing of platform termination by drowning, backstep geometries, pinnacle development, and overall platform thickness. The timing of siliciclastic basin fill dictated differences in platform-margin geometries such as slope angle, relief above basin floor, and the presence or absence of basinward platform progradation. Despite the dramatic differences in platform architecture, eustatic sea level fluctuations imparted a basinwide sequence-stratigraphic signal.

INTRODUCTION

Tectonic subsidence is regarded as a first-order mechanism controlling carbonate-platform evolution by providing antecedent topography for the nucleation of carbonate sedimentation, creating accommodation space for carbonate-sediment accumulation, influencing platform-margin geometry, and terminating carbonate sedimentation by drowning. Additional first-order mechanisms include organic evolution, eustatic sea level change, climate change, siliciclastic sediment flux, and seawater chemistry. Because all of these factors influence platform evolution and because some act independently and others are linked, it is difficult to unravel the degree to which the various factors impact the evolution of a particular platform. Our approach has been to evaluate and separate local and regional controls, such as tectonic subsidence and siliciclastic flux, from basinwide controls, such as eustasy, through comparisons among different platforms with coeval sequences constrained by biostratigraphy and chronostratigraphy.

Numerous studies have addressed the impact of tectonics on carbonate-platform evolution. Subsurface studies enable a regional evaluation of carbonate-platform architecture and the function of tectonics in providing antecedent topography for nucleation sites, in segmentation and coalescence of platforms, for development of backstepping geometry, for modification of sequence-stratigraphic patterns, and in submergence and drowning (e.g., Eberli and Ginsburg, 1987; Greenlee and Lehmann, 1993; Saller et al., 1993; Dorobek, 1995; Schlager et al., 1998; Al-Tawil et al., 2003; Weber et al., 2003). Outcrop studies have documented the impact of tectonism on particular aspects of carbonate sedimentation, for example, platform termination, syndepositional faulting, and response of depositional sequences to migrating depocenters (e.g., Dorobek et al., 1991; Giles and Dickinson, 1995; Proust et al., 1998; Smith and Read, 2001). In few cases, however, is outcrop quality sufficient to enable a basinwide evaluation of tectonic subsidence and its impact on carbonate-platform architecture. Spectacular surface exposures in the Nanpanjiang Basin of south China allow basinwide documentation of the architecture and evolution of several isolated carbonate platforms. Assessment of regional subsidence patterns is permitted by the long marine history of the basin (Proterozoic to Late Triassic), structures that expose the stratigraphic record to basement, and a high-quality stratigraphic and biostratigraphic database developed by the Guizhou and Guangxi geologic surveys.

Because carbonate sedimentation thrives in areas with limited clastic flux, carbonate platforms typically develop in passive margin and cratonic basins. The geologic record, however, contains numerous examples of carbonate ramps and platforms developed in foreland basins or basins that evolved from passive margin to foreland settings (e.g., Dorobek, 1995). Conversion to a convergent setting is particularly important for petroleum exploration because accelerated subsidence can lead to the development of aggrading and backstepping isolated platforms, forming thick reservoirs subsequently buried by clastics to form stratigraphic traps (cf. Greenlee and Lehmann, 1993). Foreland-basin models predict carbonate platforms with homoclinal ramp geometry developed on low depositional gradients produced by lithospheric flexure on the distal, cratonward side of the foreland (Dorobek, 1995). Migration of the foreland flexure toward the craton, high rates of tectonic subsidence, and migration of the peripheral bulge result in backstepping or drowning of platforms and regional topographic inversion (Giles and Dickinson, 1995). Platform evolution in convergent basins, however, may be much more diverse and complex than predicted by conceptual models. For example, high-relief platforms of diverse architectures are also possible in polytectonic basins that convert from an extensional to a convergent tectonic regime. Moreover, the influence of within-plate stress and reactivation of preexisting basement structures (Dorobek, 1995) and dynamic topography associated with a subducting slab (Gurnis, 1992, 1993) may affect complex patterns of subsidence and platform architecture hundreds of kilometers cratonward of the convergence zone.

The purpose of this article is to document the history and stratigraphic architecture of four isolated carbonate platforms in the Nanpanjiang Basin of south China, to evaluate their evolution in the context of tectonic-subsidence patterns, and to present a comparative analysis of their evolution. Isolated platforms of the Nanpanjiang Basin began in the Early Triassic in a passive-margin setting with a structural grain perhaps inherited from Paleozoic rifting. Later, the basin converted to a foreland system as south China entered into tectonic convergence and continental collision from several directions. Tectonic-subsidence rates accelerated in the Early and Middle Triassic, with earlier onset and higher rates in the southern part of the basin. The rates, magnitude, and patterns of subsidence are consistent with foreland-basin development (cf. Allen et al., 1986). Felsic volcanics thicken into the southern part of the basin. These observations point toward Triassic convergence and foreland subsidence associated with a volcanic arc developed to the south of the basin. Platform evolution responded to tectonic subsidence in a predictable pattern of backstepping and drowning. The timing of synorogenic siliciclastic turbidite fill influenced basin-floor bathymetry and, thus, platform-margin geometry. This study provides important outcrop examples of carbonate-platform evolution

from New Mexico State University. He joined Shell Exploration and Production Company in 2005, where he works as an exploration geologist for onshore United States. His interests are sedimentary geology, stratigraphy, and structural geology.

Jordayna Druke ~ *Department of Geology, University of Wisconsin–Oshkosh, Oshkosh, Wisconsin 54901; present address: Hess Corporation, Houston, Texas 77002*

Jordayna Druke received her bachelor's degree from the University of Wisconsin–Oshkosh and her M.S. degree is in progress from New Mexico State University. She recently joined Hess Oil Corporation. Her interests are sedimentary geology, sequence stratigraphy, and salt tectonics.

Benjamin Kessel ~ *Department of Geology, University of Wisconsin–Oshkosh, Oshkosh, Wisconsin 54901; present address: Anadarko Petroleum Corporation, Houston, Texas 77251*

Benjamin Kessel received his bachelor's degree from the University of Wisconsin–Oshkosh and his M.S. degree from Utah State University. He joined Anadarko Petroleum Corporation in 2005 and is currently working as a development geologist in the Rockies Conventional Group. His interests are stratigraphy, sedimentary geology, and regional and global tectonics.

Trent Newkirk ~ *Department of Geology, University of Wisconsin–Oshkosh, Oshkosh, Wisconsin 54901; present address: Newmont Mining Company, Elko, Nevada 89803*

Trent Newkirk received his bachelor's degree from the University of Wisconsin–Oshkosh and is currently working on his M.S. degree from Northern Arizona University and works at the Newmont Mining Company as a geologist on the Carlin Trend, developing underground economic potential. His interests are volcanology, volcaniclastic sedimentation, sedimentary geology, and emplacement processes.

ACKNOWLEDGEMENTS

This research is based on work supported by the National Science Foundation (EAR-9804835 to D. J. Lehrmann and EAR-9805731 to P. Enos) and by the Petroleum Research Fund of the American Chemical Society (ACS-40948-B2 and 33122-B8 to D. J. Lehrmann and ACS-34810-AC8 and 37193-AC8 to P. Enos). We thank M. A. Kominz for providing the subsidence program used in this study and for assisting us in the use of the program. This research has benefited from the extensive involvement of undergraduate students as they completed independent research studies at the University of Wisconsin–Oshkosh. We thank the University of Wisconsin–Oshkosh for supporting the undergraduate research.

DATASHARE 22

Datashare Table 1 is accessible in an electronic version on the AAPG Web site as Datashare 22 at ⟨www.aapg.org/datashare/index.html⟩.

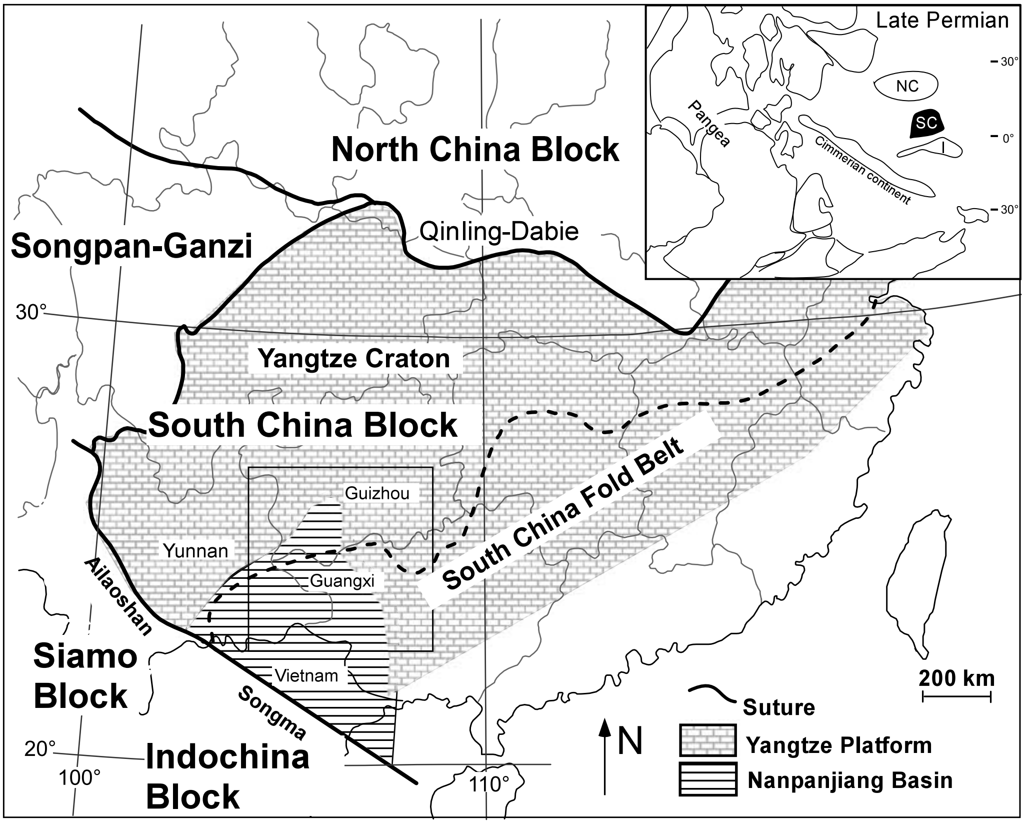

Figure 1. Tectonic map illustrating cratonic blocks (plates) of south China, interpreted suture zones, and the extent of the Nanpanjiang Basin and Yangtze platform. The South China block includes the Yangtze craton and the South China fold belt. The dashed line separating these areas is the suture proposed by Hsü et al. (1988). Modified from Sun et al. (1989). Inset, upper right, illustrates the global plate reconstruction and position of the South China block (SC), North China block (NC), and Indochina block (I) in the Late Permian. Modified from Metcalfe (1996), with permission from the Geological Society Publishing House.

in an active tectonic setting. Isolated platforms, especially those in tectonically active basins, are prime targets for hydrocarbon exploration.

GEOLOGIC SETTING

The Nanpanjiang Basin has the longest marine history of any basin in China, having been the site of marine sedimentation during most of the Late Proterozoic through Late Triassic (Enos, 1995). During the Permian and Triassic, the Nanpanjiang Basin formed a deep-marine embayment in the southern margin of the South China block (Figure 1). The South China block includes the Yangtze craton and South China fold system (Figure 1). Most authors have considered the South China block as a single continental plate that stabilized in the Proterozoic or early Paleozoic (Lin et al., 1985; Chen et al., 1991; Gilder et al., 1995; Metcalfe, 1996; Tan et al., 2000). In contrast, Hsü et al. (1988) proposed that the South China fold system is a separate tectonic block, the Huanan terrane, that united with the Yangtze craton during the Late Triassic Indosinian orogeny. This hypothesis was based on the reinterpretation of the Banxi Group as a Mesozoic mélange and implies a suture through the northern part of the Nanpanjiang Basin (Figure 1). Several authors have presented compelling evidence that the Banxi Group is part of the Proterozoic basement and, thus, reject Mesozoic suturing of the South China fold system (Gupta, 1989; Rodgers, 1989; Rowley et al., 1989; Tan et al., 2000). The stratigraphic similarities among carbonate platforms that developed across the basin, as well as similarities in subsidence histories presented herein, support the interpretation that the South China block was unified before the early Paleozoic.

The South China block is bordered on the north by the Qinling-Dabie orogenic belt, a suture between the North and South China blocks (Figures 1, 2) (Metcalfe, 1996, among many others). To the northwest, it borders the Songpan-Ganzi fold system, interpreted to be a remnant oceanic basin filled with Triassic flysch during suturing of the North and South China blocks (Sengör, 1987; Ingersoll et al., 2002; but see Enos, 1995). The South China block is bordered on the south and southwest by the Ailaoshan and Songma faults, which have been interpreted as suture zones bounding the Siamo-Sibumasu and Indochina plates, respectively (Figures 1, 2) (Klimetz, 1983; Zhang et al., 1984; Metcalfe, 1996). Plate reconstructions indicate that the South China

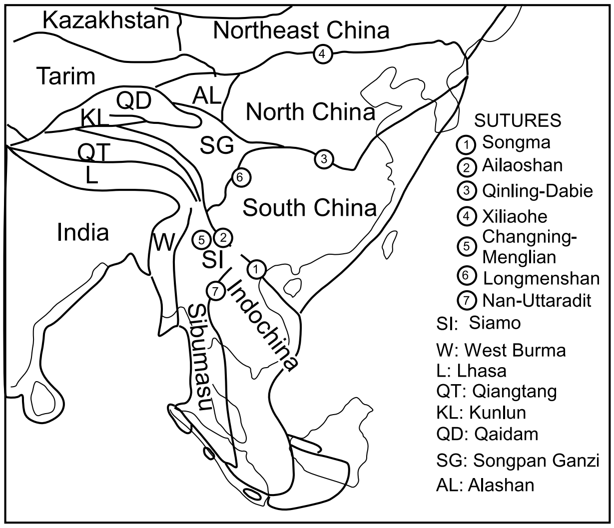

Figure 2. Tectonic plates and interpreted suture zones of China and Southeast Asia. Modified from Metcalfe (1996), with permission from the Geological Society Publishing House.

block rifted from the northeast margin of Gondwana, probably adjacent to Australia, during the Devonian (Metcalfe, 1996), drifted northward across the eastern Tethys, crossing the equator during the Permian to approximately 12°N latitude by the beginning of the Middle Triassic, and eventually docked with the North China plate along the Qinling-Dabie suture during the Late Triassic (Klimetz, 1983; Sengör, 1987; Enkin et al., 1992; Van der Voo, 1993, Enos, 1995; P. Montgomery, 2002, personal communication). Controversy regarding whether the North and South China blocks docked instead during the early Paleozoic (cf. Zhang et al., 1997) seems to have been reconciled with a tectonic model that includes earlier docking of a terrane along a northern Qinling suture followed by Late Triassic docking of the South China block along a southern Qinling-Dabie suture (cf. Meng and Zhang, 1999).

The Siamo-Sibumasu and Indochina blocks converged and collided with the southern margin of the South China block sometime during the late Paleozoic or Triassic (Figure 2) (Klimetz, 1983; Zhang et al., 1984; Fan and Zhang, 1994; Metcalfe, 1996, 2002). Controversy abounds as to the timing of suturing of the Indochina and Siamo-Sibumasu blocks to the South China block and as to whether the Songma fault zone represents a suture or a transform (Figure 2) (Findlay and Trinh, 1997). Most authors have interpreted collision and suturing along the Ailaoshan and or Songma zones during the Triassic Indosinian orogeny (Klimetz, 1983; Zhang et al., 1984; Sengör, 1987; Fan and Zhang, 1994; Carter et al., 2001). Others have postulated a Paleozoic docking of Indochina and South China blocks (Hutchinson, 1989; Metcalfe, 1996, 2002; Findlay and Trinh, 1997). The Ailaoshan and Songma zones are exceedingly complex. They may include a history of docking of smaller Paleozoic terranes in the late Paleozoic (cf. Metcalfe, 2002), as well as having been involved in Triassic convergent tectonism and metamorphism (cf. Lepvrier et al., 1997; Lacassin et al., 1998). Finally, they were overprinted by extensive Cretaceous–Tertiary shearing and metamorphism associated with India–Asia collision (cf. Tapponier et al., 1990; Lepvrier et al., 1997). Depositional patterns, subsidence history, and volcanics in the Nanpanjiang Basin presented herein point to Triassic convergence along the southern margin of the South China block.

The Nanpanjiang Basin formed a deep-marine embayment along the southern margin of the Yangtze platform, a vast area of primarily shallow-marine deposits that stretches across much of the South China block (Figure 1) (Wang, 1985; Liu and Xu, 1994; Enos, 1995; Xu et al., 1996). During the long history of marine sedimentation from the Proterozoic to the Late Triassic, the Yangtze platform–Nanpanjiang Basin system of Guizhou and Guangxi underwent several important phases of tectonic reorganization.

The South China block (Yangtze craton) stabilized during the Neoproterozoic Yangtze orogeny, which was followed by stable cratonic sedimentation during the latest Proterozoic (Sinian) and early Paleozoic (Huang, 1978; Ren et al., 1987; Metcalfe, 1996). In Guizhou and Guangxi, the Proterozoic basement is unconformably overlain by Neoproterozoic (lower Sinian) glacial and glacial-marine deposits followed in the upper Sinian and Cambrian by shallow- and deep-marine clastics marking the transgression and initiation of passive-margin sedimentation (Guangxi Bureau of Geology and Mineral Resources, 1985; Guizhou Bureau of Geology and Mineral Resources, 1987). Lower Paleozoic facies are dominated by mature clastics and shallow-marine carbonates, indicating vast and long-standing epeiric or passive-margin sedimentation (Wang, 1985).

The region became tectonically active during the Early Devonian Guangxi orogeny, resulting in the development of a basinwide unconformity and the regional absence of basal Devonian strata (Guangxi Bureau of Geology and Mineral Resources, 1985; Guizhou Bureau of Geology and Mineral Resources, 1987; Liu and Xu, 1994). The unconformity bevels the strata down to the Cambrian in southern Guangxi (Guangxi Bureau of Geology and Mineral Resources, 2000). Regional tectonic syntheses have inferred extensional block faulting during this orogeny (Qing et al., 1991). The Guangxi

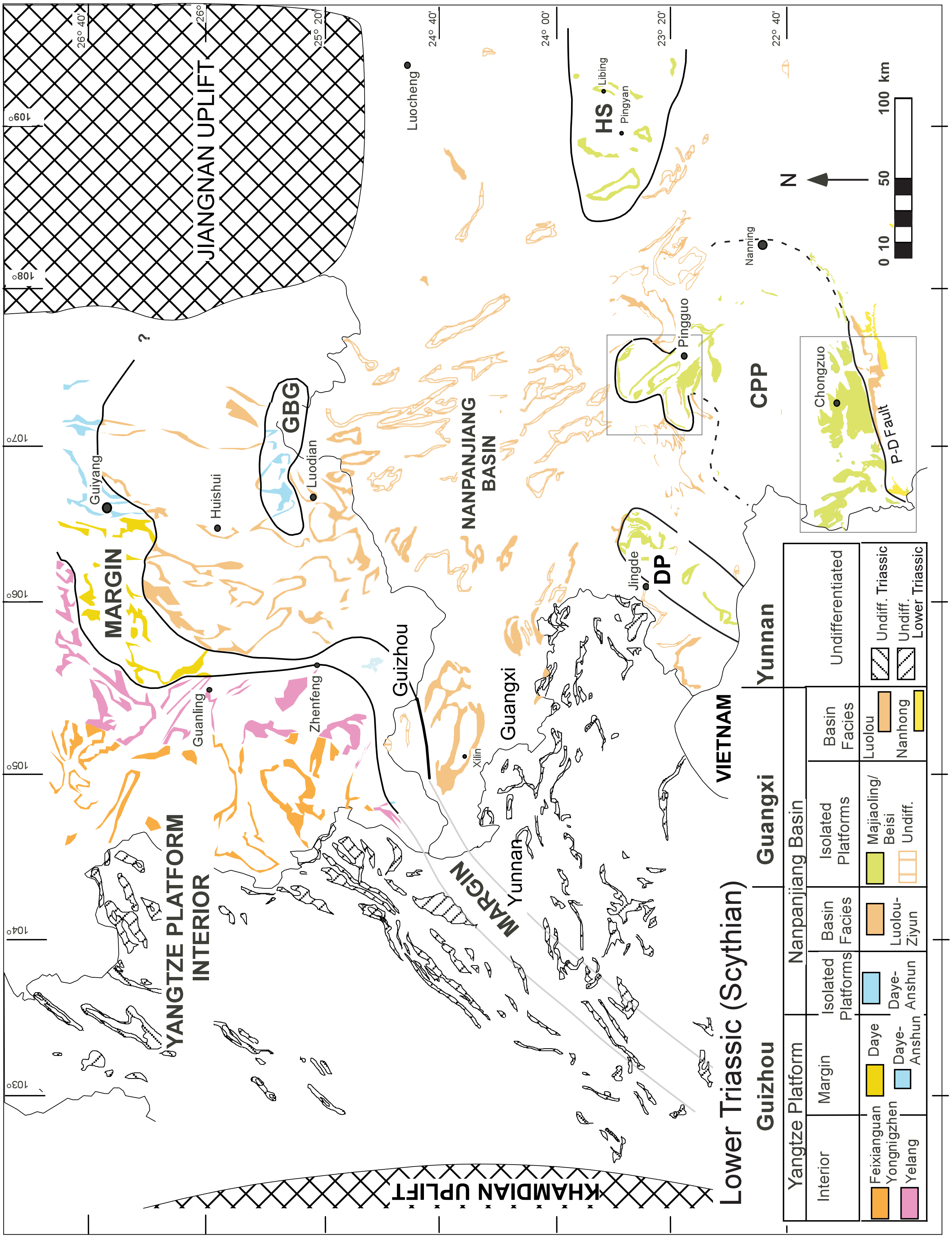

Lower Triassic (Scythian)
JIANGNAN UPLIFT
KHAMDIAN UPLIFT
YANGTZE PLATFORM INTERIOR
MARGIN
NANPANJIANG BASIN
GBG
CPP
HS
DP
P-D Fault
Guiyang
Huishui
Luodian
Guanling
Zhenfeng
Xilin
Jingde
Pingguo
Nanning
Chongzuo
Luocheng
Pingyan
Libing
Guizhou
Guangxi
Yunnan
VIETNAM
26° 40'
26°
25° 20'
24° 40'
24° 00'
23° 20'
22° 40'
103°
104°
105°
106°
107°
108°
109°
N
0 10 50 100 km
Yangtze Platform
Nanpanjiang Basin
Interior
Margin
Isolated Platforms
Basin Facies
Undifferentiated
Feixianguan Yongnigzhen
Yelang
Daye
Daye-Anshun
Luolou-Ziyun
Majiaoling/Beisi
Undiff.
Luolou
Nanhong
Undiff. Triassic
Undiff. Lower Triassic

orogeny has been widely attributed to the extensional deformation overprinting the region (Huang, 1978; Guangxi Bureau of Geology and Mineral Resources, 1985; Guizhou Bureau of Geology and Mineral Resources, 1987; Qing et al., 1991; Xu et al., 1996). Plate reconstructions indicate that Early Devonian uplift and extension resulted from the rifting of the South China block from Gondwana (cf. Metcalfe, 1996).

Passive-margin deposition resumed in the late Paleozoic, with widespread development of shallow-marine carbonate sedimentation in the Yangtze platform in Guizhou and around the eastern periphery of the Nanpanjiang Basin in Guangxi (Wang, 1985; Enos, 1995; Xu et al., 1996). Regional paleogeographic reconstructions indicate that isolated carbonate platforms developed within the basin in Guangxi beginning in the Devonian (Wang, 1985; Xu et al., 1996). Some authors have speculated that horst blocks, formed in the Devonian, established the structural grain for the nucleation of isolated carbonate platforms in Guizhou and Guangxi (cf. Qing et al., 1991). Regional mapping demonstrates that the margin of at least one of the isolated Triassic platforms, the Chongzuo platform in the southern part of the basin, was controlled by a fault, and that another, the Great Bank of Guizhou in the northern part of the basin, nucleated on antecedent topography of a subtle arch or an Upper Permian reef margin instead of a fault block (Figure 3) (Lehrmann et al., 1998).

The Lower to Upper Permian transition is marked by a period of renewed tectonic activity with extensional faults, the eruption of the Emeishan Basalt along the western margin of the basin, and the development of a disconformity that extends across the entire basin (Guangxi Bureau of Geology and Mineral Resources, 1985; Guizhou Bureau of Geology and Mineral Resources, 1987). This period of activity is referred to as the Dongwu movement in the Chinese literature (Zhang, 1984; Guizhou Bureau of Geology and Mineral Resources, 1987; Huang and Chen, 1987). The most dramatic expression of this tectonism is the vast outpouring of the Emeishan Basalt. The basalt eruption was apparently centered in southwestern Sichuan and eastern Yunnan, where maximum reported thicknesses exceed 2 km (1.2 mi) (Luo et al., 1990; Chung and Jahn, 1995). Emeishan volcanism has been variously interpreted as the result of rifting, back-arc spreading, or the development of a mantle plume (Guizhou Bureau of Geology and Mineral Resources, 1987; Luo et al., 1990; Qing et al., 1991; Xu et al., 1996; Song et al., 2004). The Emeishan Basalt has a maximum thickness of 550 m (1804 ft) in western Guizhou. The basalt thins and pinches out to the southeast and is found only within the westernmost part of the Nanpanjiang Basin, indicating that the Dongwu movement had its greatest impact on the western part of the basin.

From the Late Permian to the Middle Triassic, the Yangtze platform was the site of a thick and expansive succession of shallow-marine carbonates with intermittent siliciclastic influx from the west and with a variety of ramp, reef, and collapsed platform margins (Enos, 1995; Enos et al., 1997, 1998, in press). Isolated carbonate platforms developed within the basin during the Triassic (Figure 3) (Lehrmann et al., 1998). Deep-marine sedimentation in the Early Triassic basin was dominated by relatively thin starved pelagic carbonate and shale of the Luolou Formation (Figure 3), indicating tectonic quiescence.

Conditions changed radically during the Middle and Late Triassic. The basin rapidly subsided and was eventually filled with siliciclastic turbidites (Figures 3–5). Carbonate platforms were progressively drowned and buried by siliciclastics, from the beginning of the Middle Triassic (Anisian) in the southern basin to the early Late Triassic in the northern basin (Figures 3–5). Marine turbidites were succeeded by Norian shallow-shelf and fluvial siliciclastics, marking the end of marine sedimentation in south China (Enos et al., 1998). These changes record the Indosinian orogeny in the Nanpanjiang Basin and Yangtze platform (Enos et al., in press). The specific tectonic cause is still unclear because of uncertainty of the timing and patterns of convergence of tectonic collage that make up China (Figure 2).

The Triassic Nanpanjiang Basin has been variously interpreted as a foreland basin with an arc developed either in southern Guangxi or within an adjacent

Figure 3. Lower Triassic (Scythian) lithofacies and interpreted paleogeography of the Nanpanjiang Basin and Yangtze platform in parts of Guizhou, Guangxi, and Yunnan. Compiled from the regional geologic maps of the Yunnan Bureau of Geology and Mineral Resources (1984), Guangxi Bureau of Geology and Mineral Resources (1985), Guangxi Bureau of Geology and Mineral Resources (2000), and Guizhou Bureau of Geology and Mineral Resources (1987). Maps have been modified with results from our mapping. Data control (colored facies polygons) is the distribution of surface exposure of various facies (formations) indicated in the legend. GBG = Great Bank of Guizhou; DP = Debao platform; HS = Heshan platform; CPP = Chongzuo-Pingguo platform. Gray rectangles in Chongzuo and Pingguo areas indicate areas of detailed maps in Figures 6 and 8, respectively. Subareas of the basin used for subsidence analysis are centered in Guiyang, Guanling, Zhenfeng, Huishui, Luodian, Luocheng, Pingguo, and Chongzuo.

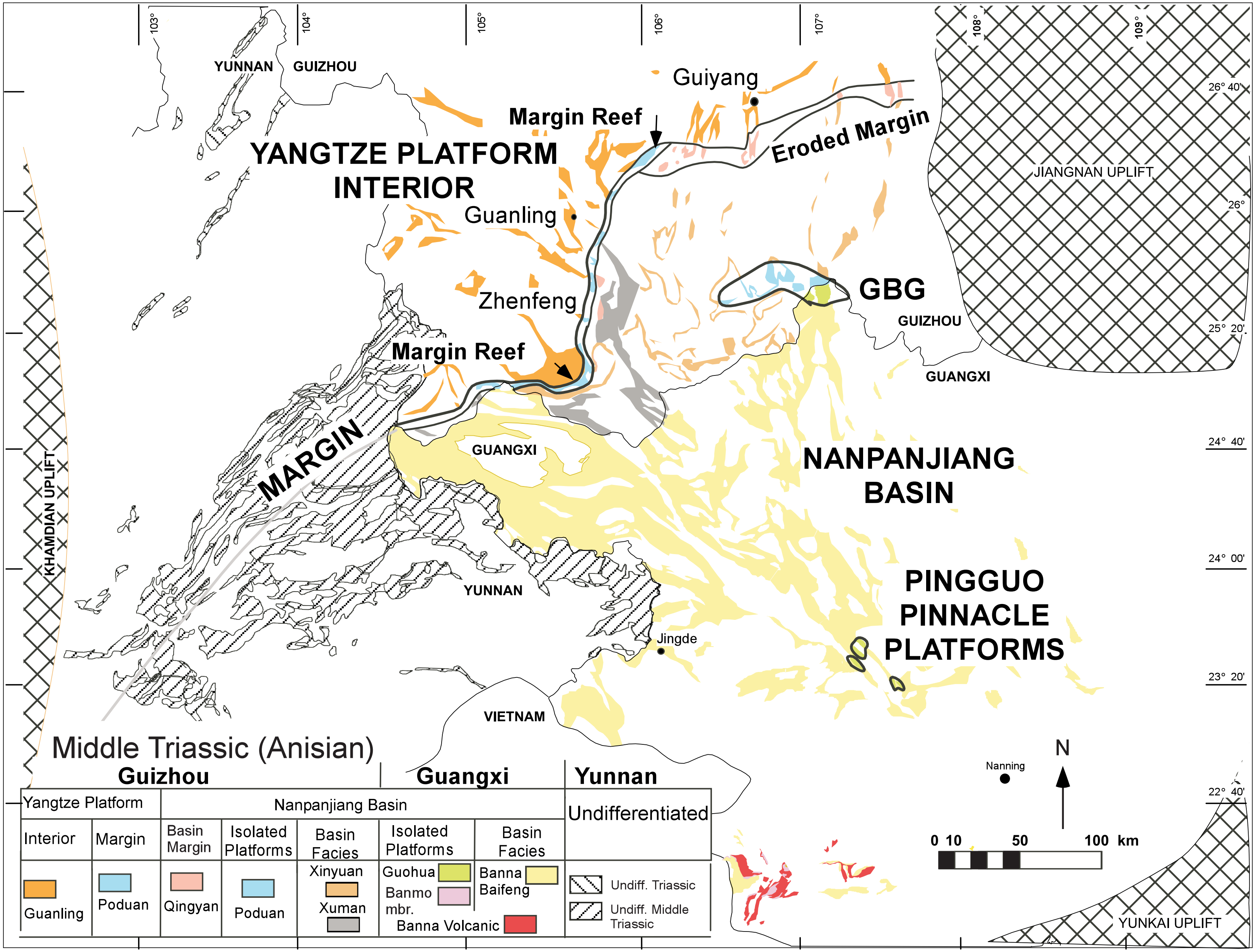

Figure 4. Middle Triassic (Anisian) lithofacies and interpreted paleogeography of the Nanpanjiang Basin and Yangtze platform in Guizhou, Guangxi, and Yunnan. Compilation data and methods are given in the caption of Figure 3. GBG = Great Bank of Guizhou.

continent (He, 1986; Xia et al., 1993), as a back-arc extensional basin (Hou and Huang, 1984), as a foreland basin developed along the eastern side of the collision zone along the Ailaoshan suture (Qing et al., 1991), and as a flysch nappe thrust over a suture zone from the Huanan block onto the Yangtze craton (Hsü et al., 1988). Triassic history suggests that the Nanpanjiang Basin was a foreland basin, specifically a perisutural basin that developed on the continental lithosphere associated with compressional tectonics (Allen et al., 1986) because the South China block was involved in convergence and collision, probably along its southern, northern, and western sides. Enos et al. (1998, in press) noted that the facies succession that formed during the termination of the Yangtze platform forms a classic flysch to molasse sequence typical of a foreland basin. However, the source orogen and transport directions of the siliciclastics remain poorly understood.

METHODS

Paleogeographic maps representing Early Triassic and two Middle Triassic (Anisian and Ladinian) time slices for the Nanpanjiang Basin were constructed by digitizing outcrop areas of formations from regional geological maps of Guizhou, Guangxi, and Yunnan provinces at scales of 1:500,000 or 1:1,000,000 (Yunnan Bureau of Geology and Mineral Resources, 1984; Guangxi Bureau of Geology and Mineral Resources, 1985; Guizhou Bureau of Geology and Mineral Resources, 1987; Guangxi Bureau of Geology and Mineral Resources, 2000), modified with observations from our mapping from 1988 to 2001 (Figures 3–5). Chinese regional mapping defines most formations to coincide with stage boundaries. For each stage, formations were defined representing platform-margin, platform-interior, basin, and, locally, basin-margin lithofacies, thus facilitating the construction of paleogeographic maps (cf. Figures 3–5). Four isolated carbonate platforms were thus defined from regional geologic maps (Figures 3–5). Each of the platforms has some unconstrained margins and, thus, could possibly be attached to a landmass. However, they lack any shallow-marine siliciclastics or other evidence of terrestrial influence, indicating that they were isolated platforms (cf. Lehrmann et al., 1998).

Carbonate-platform architecture was constrained by the detailed mapping of two-dimensional (2-D) cross sections on the steeply dipping limbs of faulted synclines that dissect the platforms. Northwest-trending Cretaceous and Cenozoic folds dissect the Great Bank of Guizhou and Pingguo platform areas (Figure 3) to provide continuously exposed, 2-D cross sections through the platform interior and margins (cf. Lehrmann et al., 1998). The Chongzuo platform area in southern Guangxi is dissected by numerous faults. The architecture of this area was reconstructed by reconnaissance mapping and measured sections. The longest and most important of these sections include three in the platform interior and two in the basin margin (Figures 6, 7). A broad outline of the architecture of the Heshan and Debao platforms was documented through reconnaissance mapping and through a detailed description of critical horizons, such as drowning surfaces. In the Chongzuo-Pingguo and Heshan areas, approximately 7 km (4.3 mi) of stratigraphic section was described at a scale of 1:100 and sampled. Numerous detailed sections were described at a scale of 1:25 to evaluate facies succession across critical intervals such as backstep and termination horizons. The architecture and evolution of the Great Bank of Guizhou was documented through mapping and description of approximately 5 km (3.1 mi) of stratigraphic section (Lehrmann et al., 1998).

Chronostratigraphic correlation was accomplished through conodont, ammonoid, and foraminifer biostratigraphy. The bulk of our biostratigraphy was done with conodonts, primarily from basin-margin successions and from platform-interior–flooding horizons and platform-drowning horizons. Several volcanic-ash beds bracket the Permian–Triassic and Lower–Middle Triassic boundaries. These volcanic horizons form excellent chronostratigraphic markers and were dated using U-Pb radioisotopes (S. Bowring, 2006, personal communication; Lehrmann et al., 2006).

Magnetic susceptibility profiles were used in the correlation of sections within the Chongzuo-Pingguo platform (CPP) (Figure 7). Magnetic susceptibility samples were taken at intervals of approximately 0.5–1 m (1.6–3.3 ft) and were measured with the susceptibility bridge at Louisiana State University, using the techniques described in Ellwood et al. (1999). Magnetic susceptibility is a function of the concentration of detrital ferric-iron minerals and is controlled by fluctuations in flux of lithogenic material, which responds to both climate change and sea level change. Magnetic susceptibility signatures can be used for chronostratigraphic correlation, with the assumption that the flux of magnetic detrital grains are dispersed widely across the basin (Crick et al., 1997; Ellwood et al., 1999).

Depositional sequences were delineated from platform-margin geometries and, in platform-interior sections, from cycle-stacking patterns. Depositional

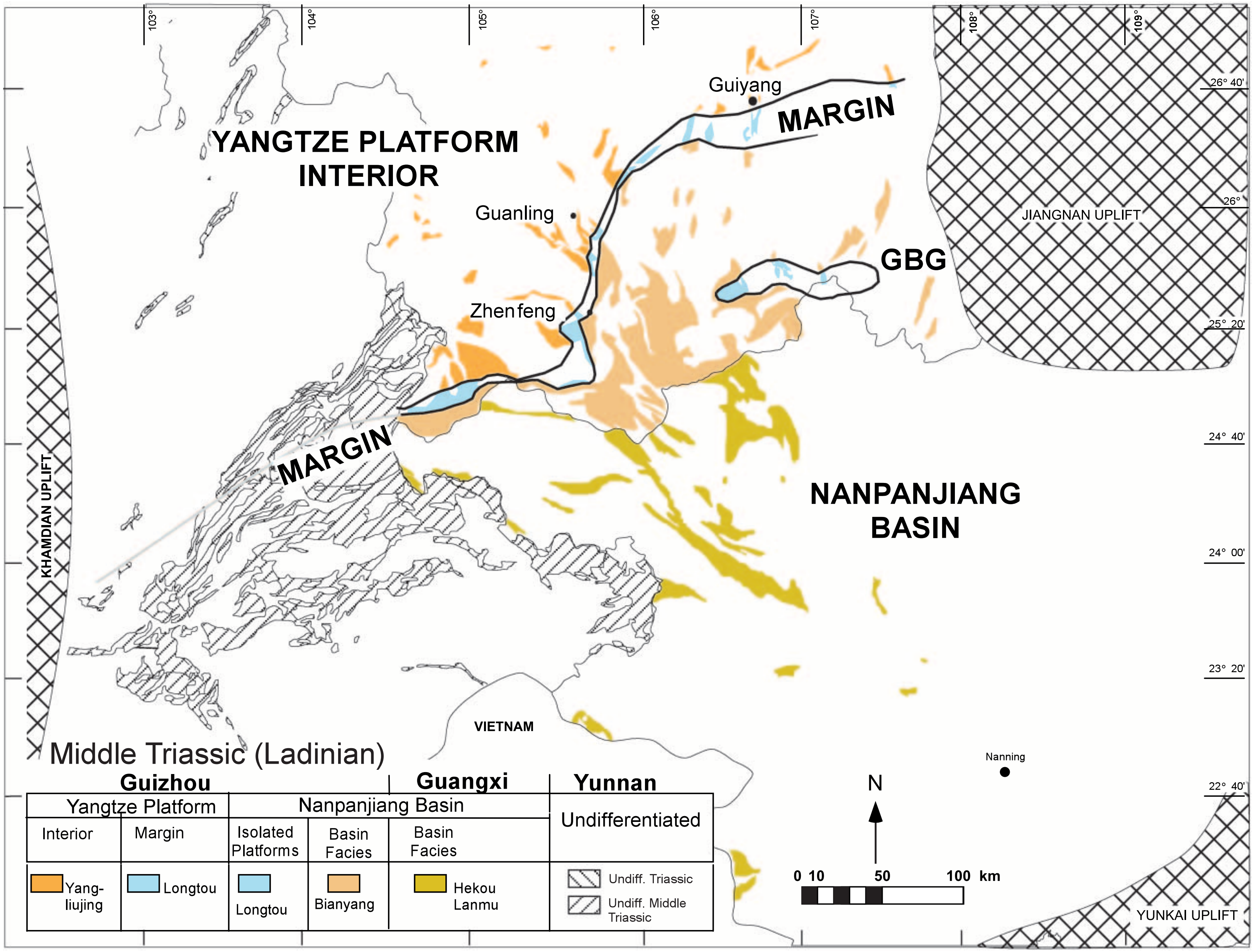

Figure 5. Middle Triassic (Ladinian) lithofacies and interpreted paleogeography of the Nanpanjiang Basin and Yangtze platform in Guizhou, Guangxi, and Yunnan. Compilation data and methods are given in the caption of Figure 3. GBG = Great Bank of Guizhou.

sequences were correlated within and between platforms in the context of biostratigraphic constraints, magnetic susceptibility profiles, and volcanic horizons.

Subsidence analysis began with the compilation of regional stratigraphic data with the assistance of geologists from the Guizhou and Guangxi geologic surveys. A table summarizing the stratigraphic data used in the subsidence analyses is included in the online AAPG Datashare (Datashare 22, http://www.aapg.org/datashare/index.html). Subregions of the basin were identified to characterize patterns in subsidence and to provide the most continuous composite sections penetrating the oldest strata possible. Sections were selected that (1) represent shallow-marine environments (to minimize errors of water-depth estimates), (2) are the most continuous (to minimize errors associated with unconformities), and (3) have the best biostratigraphic control. Water depths were estimated using facies and paleontologic evidence. Biostratigraphy and Chinese stage assignments were correlated with European stages and the geologic time scale of Ogg (2004). For Triassic intervals, we have integrated our detailed thicknesses, biostratigraphy, and age dates into the analysis. Subsidence analysis (backstripping) was performed with a program provided by M. A. Kominz using the decompaction algorithms of Bond and Kominz (1984).

CARBONATE-PLATFORM EVOLUTION

Chongzuo-Pingguo Platform

The CPP is the southernmost and largest isolated platform (Figure 3; Table 1). The platform evolved as a low-relief bank in the Early Triassic (Figure 3), was interrupted by volcanism at the end of the Early Triassic (Figures 6, 7), and backstepped and developed smaller pinnacle platforms in the Middle Triassic (Anisian, Bithynian) as the interior drowned and shifted to basinal siliciclastic deposition (Figures 4, 8–10; Table 1). The pinnacle platforms aggraded and were terminated in the Middle Triassic (Anisian, Pelsonian) (Figures 5, 10, 11; Table 1).

Lithofacies and Depositional Environments

Upper Permian Strata

The Upper Permian strata in the CPP are the Heshan and Dalong formations. The upper part of the Heshan Formation consists of cherty skeletal packstone with diverse shallow-marine biota (Table 2). The Dalong Formation is composed of dark, cherty, spiculitic mudrock, and argillaceous limestone with a deep-water fauna (Table 2). Regional maps combine the Heshan and the overlying Dalong in one map unit across much of the study area (Figure 6). However, in the Chongzuo area, the Pingxiang-Dongmen fault was upthrown on the north during the Late Permian, favoring shallow-water deposition of the Heshan Formation north of the fault and deeper water deposition of the Dalong Formation south of it (Figures 6, 7).

Permian–Triassic Boundary

The Permian–Triassic boundary in the Chongzuo and Pingguo areas has been described in detail by Lehrmann et al. (2003). The boundary is conformable in the Pingguo area, where cherty skeletal packstone of the upper Heshan Formation, with diverse open-marine fauna, is overlain by microbial carbonates (thrombolites) of the basal Majiaoling Formation (Table 2; Figure 10).

The Permian–Triassic boundary is unconformable across much of the CPP in the Chongzuo area. At sections LY and LJ, the Majiaoling Formation disconformably overlies the Upper Permian strata of the Heshan Formation (Figures 6, 7). West of the LJ section, the Majiaoling Formation overlies Lower Permian strata. The beveling of the strata into the Lower Permian suggests that the unconformity resulted from tectonic uplift. The boundary appears conformable in sections in the basin south of the Pingxiang-Dongmen fault (Figures 6, 7).

Lower Triassic Strata

Lower Triassic formations consist of shallow-marine carbonates of the Majiaoling and Beisi formations and basinal deposits of the Luolou Formation (Figure 3; Table 2). The distribution of Lower Triassic formations shown by regional geologic maps delineates the extent of the CPP (Figure 3). In the Pingguo area, platform carbonates are bounded to the north, west, and east by basinal deposits (Figure 3). The southern margin of the platform in the Chongzuo area is defined by the Pingxiang-Dongmen fault for 85 km (52 mi) as evidenced by shallow-marine formations north of the fault and basinal deposits south of it (Figures 3, 6). To the east, the margin is poorly constrained because of the lack of outcrop (Figure 3). Uplift and erosion of the Nanning anticline have largely isolated exposures of CPP carbonates in the Pingguo area from those in the Chongzuo area, but isolated outcrops west of Nanning and south and west of Pingguo indicate that it developed as a single platform (Figure 3).

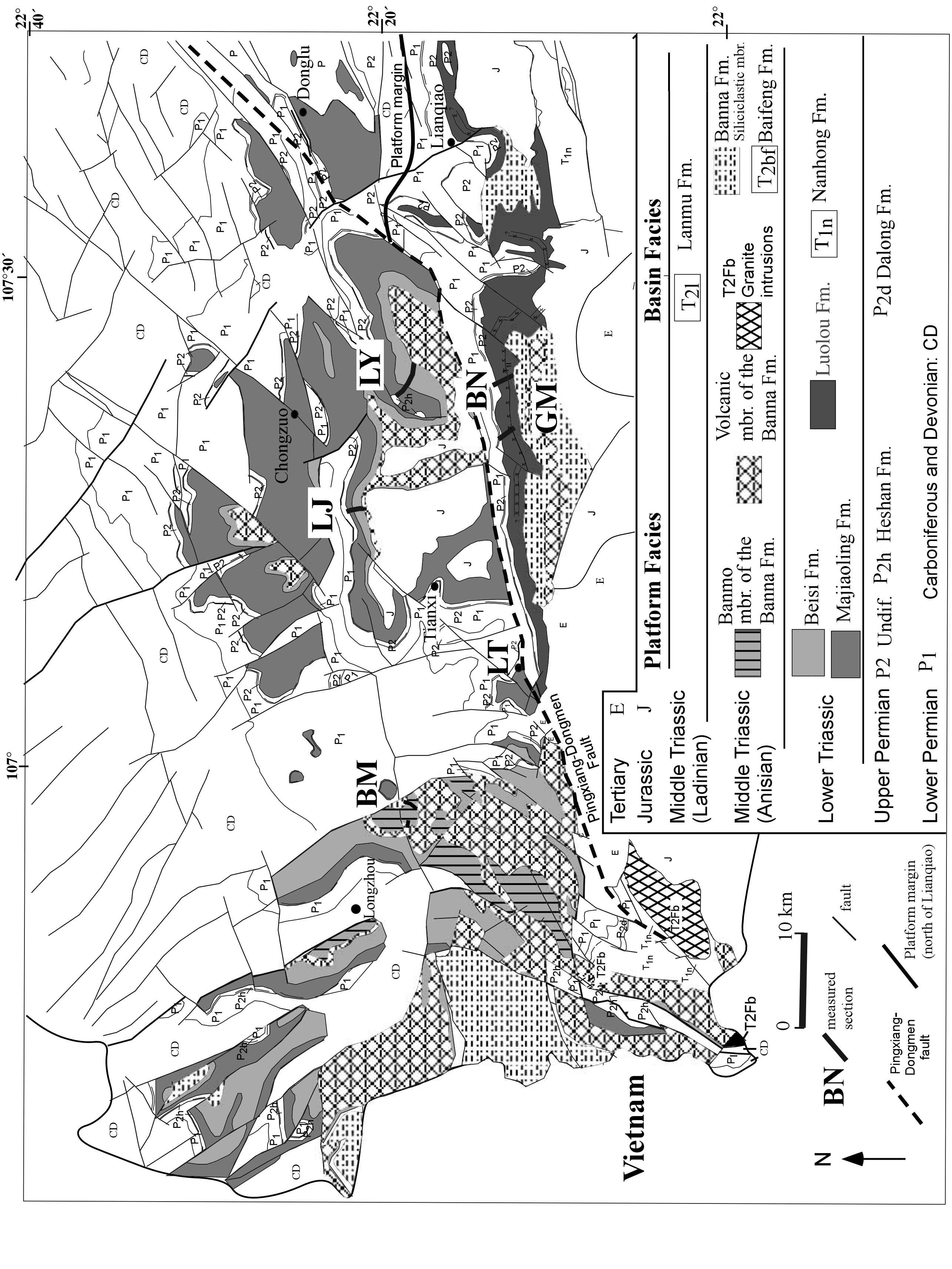
Platform Facies
Basin Facies
Tertiary E
Jurassic J
Middle Triassic (Ladinian)
T21 Lanmu Fm.
Banna Fm. Siliciclastic mbr.
T2bf Baifeng Fm.
Middle Triassic (Anisian)
Banmo mbr. of the Banna Fm.
Volcanic mbr. of the Banna Fm.
T2Fb Granite intrusions
Lower Triassic
Beisi Fm.
Majiaoling Fm.
Luolou Fm.
T1n Nanhong Fm.
Upper Permian P2 Undif. P2h Heshan Fm. P2d Dalong Fm.
Lower Permian P1
Carboniferous and Devonian: CD
22° 40´
22° 20´
22°
107°
107°30´
Vietnam
Longzhou
Chongzuo
Tianxi
Donglu
Lianqiao
Platform margin
Pingxiang-Dongmen Fault
BM
LJ
LY
LT
BN
GM
0 10 km
measured section
fault
Platform margin (north of Lianqiao)
Pingxiang-Dongmen fault
N

Lower Triassic Majiaoling Formation

The Majiaoling Formation is composed of light- to medium-gray, thin-bedded, platy lime mudstone separated by argillaceous seams (Table 2; Figures 7, 12A). Minor thin oolite beds occur in the basal 50 m (164 ft) along with thicker homogenous mudstone beds that suggest bioturbation. The low-diversity molluskan fauna is suggestive of restricted marine circulation. Oolites are interpreted to have been transported, presumably from the platform edge, during storms (Table 2).

Lower Triassic Beisi Formation

The Beisi Formation consists primarily of platy, thin-bedded lime mudstone and thick, cross-bedded oolite arranged into meter-scale cycles and larger depositional sequences 50–300 m (164–1000 ft) thick (Figures 7; 12B, C). The upper part of the formation is dolomite. The lower part of the formation contains considerable shale in the Pingguo area (Figure 11). Oolite thins into the platform interior from sections LY to LJ in the Chongzuo area (Figures 6, 7) and away from the northern margin of the platform in the Pingguo area (northwest of the TP section, Figure 10), indicating ooid shoals at the platform margin.

Thin-bedded lime mudstones are similar to those described from the Majiaoling Formation (Table 2). The mudstones are interpreted to represent deeper subtidal, transgressive parts of depositional sequences. Oolite beds range from a few decimeters thick to cliff-forming amalgamated beds up to 25 m (82 ft) thick (Figures 7, 12B). Fabrics and grain types indicate high-energy subtidal to intertidal shoals (Table 2). Included are giant ooids from 0.5 to 1 cm (0.2 to 0.4 in.) in diameter (Figure 12D). Evidence for subaerial exposure at cycle and sequence boundaries includes desiccation cracks, flaser-bedded ribbon rock (cf. Lehrmann et al., 2001), and fenestral laminites.

Facies changes within depositional sequences result in distinctive magnetic susceptibility signatures (Figures 7, 11). The transgressive argillaceous lime mudstone yields a spiky profile with high magnetic susceptibility that changes upward into a blocky profile of lower magnetic susceptibility characteristic of regressive oolite. Figures 7 and 11 illustrate our best sequence-stratigraphic and magnetic susceptibility correlation between the Chongzuo and Pingguo areas. Each of the sequences shallows upward from thin-bedded lime mudstones to thickening and coarsening oolite facies and is capped with fenestral laminite or ribbon rock. Differences in sequence development between the two areas include an interval of marine shale in the transgressive part of sequence 2 in the Pingguo area (Figure 11) and the apparent addition of sequence 2a in the Chongzuo area (Figures 7, 11). In both areas, sequences 2 and 2A contain the greatest proportion of oolite in the Beisi Formation, which is followed upward by increased proportions of lime mudstone, indicating that this interval represents a second-order highstand in sea level. Sequence 4 is overlain by felsic volcanics in both the Pingguo and Chongzuo areas (Figures 7, 11). The presence of four or five depositional sequences spanning the Lower Triassic indicates they are third order (duration of approximately 1 m.y.).

Lower Triassic Luolou Formation

The Luolou Formation spans the Lower Triassic in Guangxi and is interpreted to be the basinal equivalent of the Majiaoling and Beisi formations (Guangxi Bureau of Geology and Mineral Resources, 1985). The Luolou consists of black, laminated, pyritic lime mudstone with interbeds of shale and breccia (Table 2). The texture, sedimentary structures, and pelagic fossils indicate deep-marine, largely anoxic sedimentation (Table 2). At the basin-margin slope south of Chongzuo (Figures 6, 7), the Luolou contains slump folds and several debris-flow breccias. Breccias contain clasts derived from the platform and basin margin (Table 2) and include oolite with leached ooids and dropped nuclei, indicating meteoric dissolution at the margin prior to transport.

Middle Triassic Strata

The change in stratigraphic architecture of the CPP from the Lower to Middle Triassic is revealed by a northwest-trending fold that exposes a 2-D cross section (Figure 8). This is best visualized by viewing the strata down the structural dip on the northeast limb of the syncline (area of sections TP and NM, Figures 8, 9). Following bank development in the Lower Triassic, most of the platform shifted to deep-marine siliciclastic deposition of the Banna Formation by the Bithynian

Figure 6. Geologic map of the Chongzuo area. Modified from Guangxi Bureau of Geology and Mineral Resources (2000, scale 1:500,000), using field observations made by P. Donghong (unpublished data). The map area is indicated in Figure 3. Sections BM, LJ, LY, GM, and BN are presented in Figure 7. The southern margin of the platform coincides with the Pingxiang-Dongmen fault, except where it continues south of the fault in the eastern part of the map area north of Lianqiao.

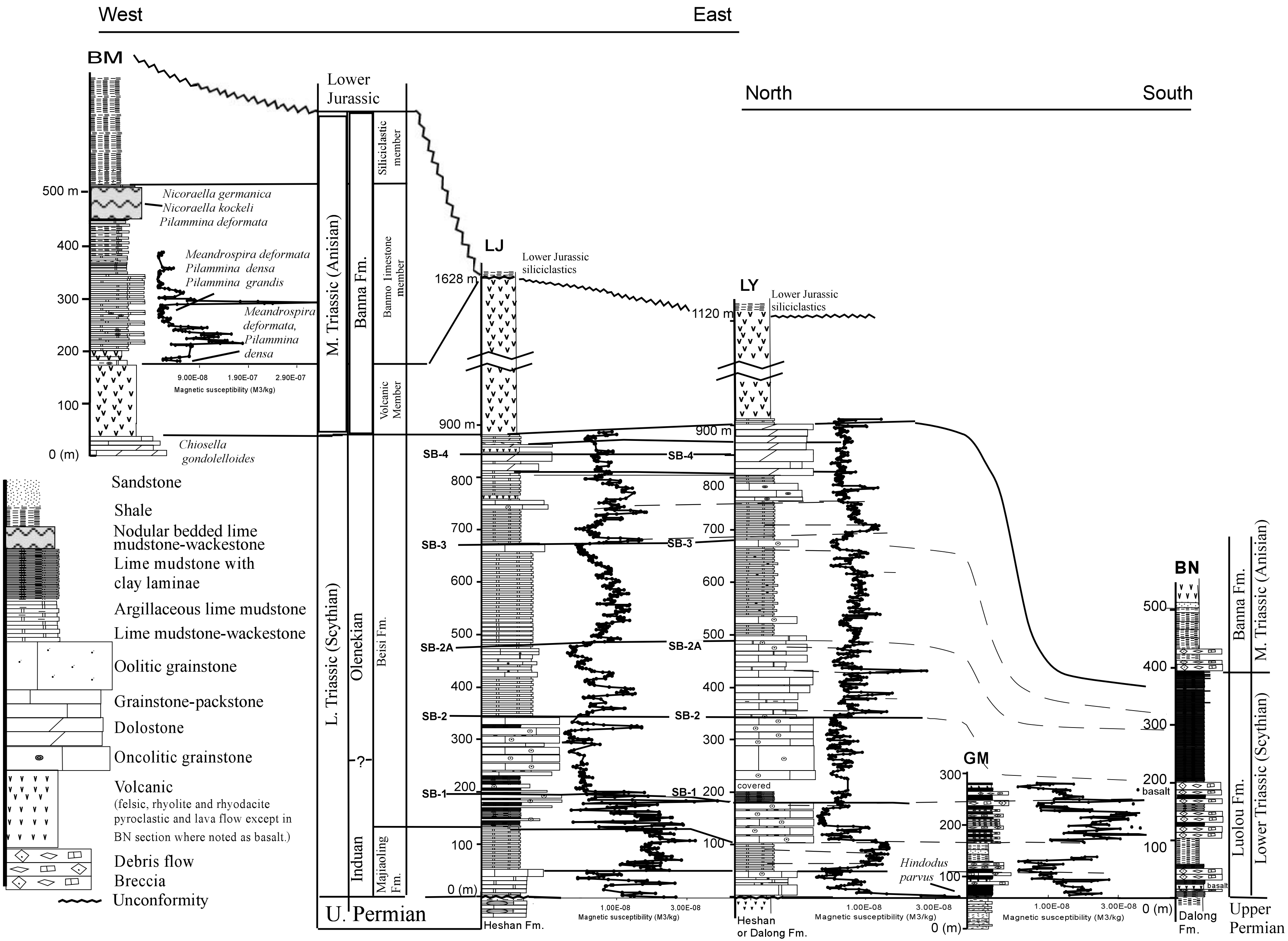

Figure 7. Stratigraphic cross section of the Chongzuo area. Stratigraphic sections BM, LJ, and LY occur within the platform; BN and GM at the basin margin (Figure 6). SB-1 to SB-4 are sequence boundaries.

Table 1. Comparison of Platform Architecture and Evolution

Platform, Size, and Architecture	Ages*	Phases of Platform Evolution (Formation Thickness)	Sequences and Flooding Events
CPP: >18,000 km^2 (6949 mi^2); Backstepped low-relief bank with smaller pinnacles (10–60 km^2; 3.8–23 mi^2)	L. P.–E. Tr.	Fault-controlled southern margin (escarpment)	
	E. Tr.–Anisian (Bithynian)	Low-relief bank with oolite at margins (900 m; 2952 ft)	1–4
	E. Tr.–Anisian boundary	Volcanic burial (up to 1640 m [5380 ft] at Chongzuo; 6 m [19 ft] at Pingguo)	
	Anisian (Bithynian)	Interior drowning, margin stepback	Max F-4
	Anisian (Bithynian–Pelsonian)	Pinnacle platforms with reefs, aggradation concurrent with basin fill (1700 m; 5577 ft)	5–6
	Anisian (Pelsonian)	Drowning and burial by basinal clastics	Max F-6
Heshan: >5000 km^2 (1930 mi^2); low-relief bank	E. Tr.	Low-relief bank with oolite margins (870 m; 2854 ft)	–
	Late E. Tr. (Spathian)	Drowning and burial by basinal clastics	–
Debao: >3000 km^2 (>1158 mi^2); low-relief bank	E. Tr.	Low-relief bank with oolite margins (506 m; 1660 ft)	–
	M. Tr.	Pinnacle platforms with reefs (known from allochthonous debris flows in basin)	–
Great Bank of Guizhou: 2000 km^2 (772 mi^2); progressively steepening megabank	L. P.	Initiated on topographic high inherited from Yangtze platform	F-1
	E. Tr.	Low-relief bank (300–500 m; 1000–1640 ft)	1–4
	E. Tr.–Anisian boundary	Volcanics (at basin margin only; <4 m [<13 ft])	
	Anisian	Progressively steepening, *Tubiphytes* reef rimmed platform (600–750 m; 1968–2460 ft)	5–6
	Ladinian	High-relief escarpment (~1900 m; ~6233 ft)	7–8
	Carnian	Drowning and burial by basinal clastics; clastics onlap escarpment	Max F-8

*L. P. = Late Permian; E. Tr. = Early Triassic; M. Tr. = Middle Triassic; Max F = maximum flooding surface.

(middle Anisian, Figures 8, 10, 11; top of TP section). Shallow-marine carbonate deposition backstepped and accumulated smaller pinnacle platforms represented by the Guohua Formation (Figures 8, 10).

Middle Triassic (Anisian) Banna Formation

The term ''Banna Formation'' is used for Middle Triassic shale and siliciclastic turbidites and for felsic volcanics in basinal settings (Guangxi Bureau of Geology and Mineral Resources, 2000); felsic volcanics on the platforms are referred to as the Beisi Formation. It appears that the felsic volcanics must be genetically related; up to 1640 m (5380 ft) of volcanics can scarcely have covered the CPP without spilling into the basin. Therefore, we refer to all of these volcanics as the volcanic member of the Banna Formation. Limestone overlies the volcanics in the Chongzuo and Pingguo areas and is overlain by the siliciclastics. These limestones are informally called the ''Banmo member,'' instead of (upper) Beisi, as in previous usage (Guangxi Bureau of Geology and Mineral Resources, 2000). Siliciclastic shale and turbidites are referred to as the siliciclastic member of the Banna Formation.

Volcanic Member

The volcanic member at the base of the Banna Formation is composed of porphyritic rhyolitic dacite and tuff (Newkirk et al., 2002). The unit is widespread in the Chongzuo area (Figure 6), with the estimated thickness ranging from 500 to 1640 m (1640 to 5380 ft)

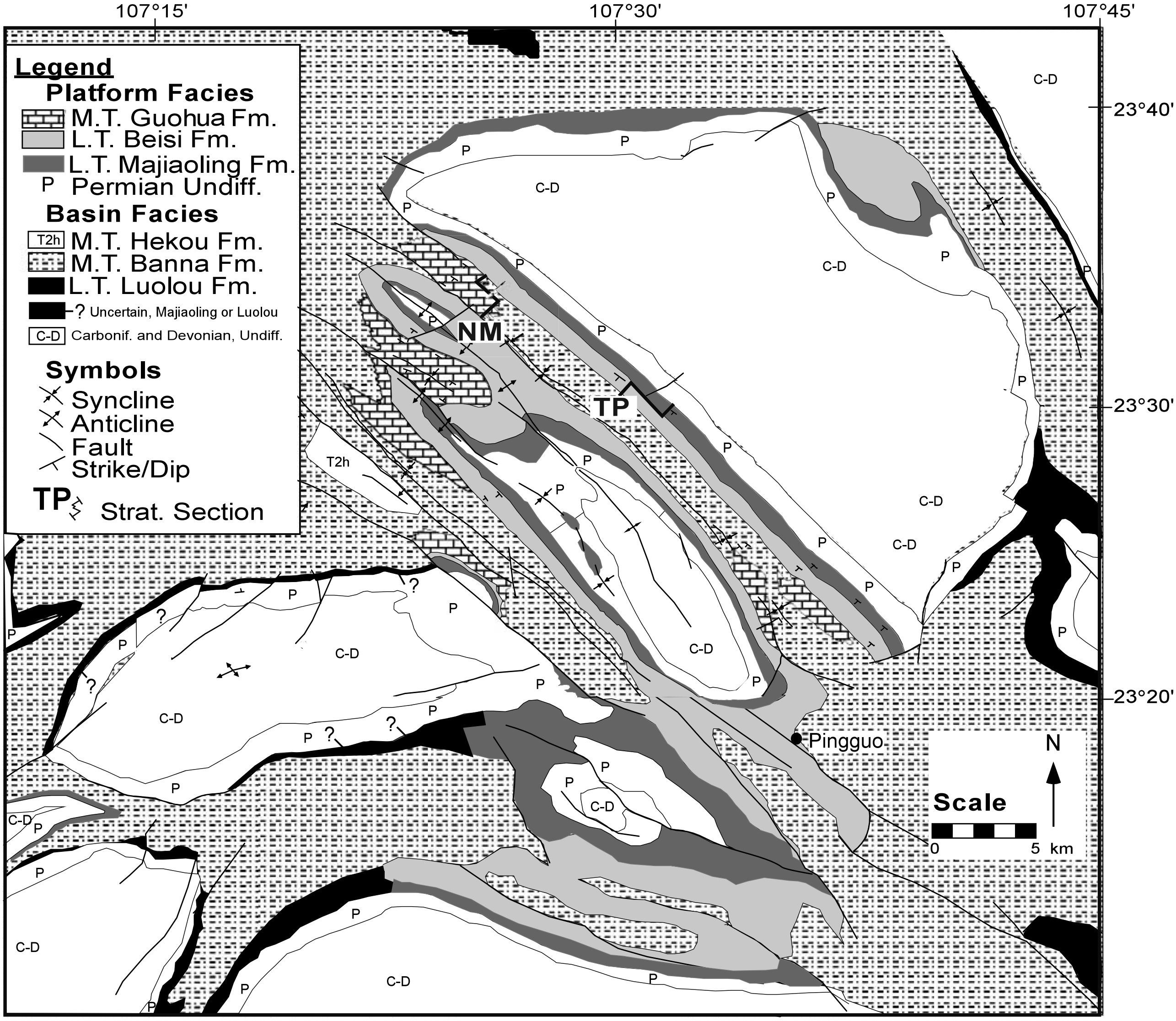

Figure 8. Geologic map of the Pingguo area. Modified, using field mapping, from Guangxi Bureau of Geology and Mineral Resources (1985, scale 1:1,000,000; 2000, scale 1:500,000) and Guangxi Bureau (unpublished geologic maps, 1975, scale 1:200,000). The map area is indicated in Figure 3. Sections TP and NM are presented in Figure 11.

(Guangxi Bureau of Geology and Mineral Resources, 2000). In the Pingguo area, the unit is only 6 m (19 ft) thick, but extends continuously across the platform (Guangxi Bureau of Geology and Mineral Resources, 1985) (Figures 10, 11). Volcanics from the Chongzuo area are interpreted as lava flows and pyroclastic tuffs based on field and petrographic observations (Table 2) (Newkirk et al., 2002). At Pingguo, the unit is interpreted to be a water-lain vitric tuff. Several lines of evidence support the correlation of the thick volcanic succession at Chongzuo, with the thinner tuff at Pingguo. (1) Biostratigraphy indicates a position near the Olenekian–Anisian boundary in both areas. *Chiosella gondolelloides*, an index fossil that straddles the upper Olenekian to the basal Anisian (Aegean–Bithynian), occurs immediately below the volcanics at Chongzuo and above the volcanics at Pingguo (Figures 7, 11). Carbonates of the Banmo member overlying the volcanics in both areas contain an assemblage of lower Middle Triassic (Bithynian) conodonts, foraminifers, and ammonoids (see next section). (2) Immobile trace-element signatures are similar in both areas, indicating a common source (Newkirk et al., 2002). (3) A preliminary zircon age for the tuff at Pingguo of ca. 247 Ma corresponds to dated tuffs just above the Olenekian–Anisian boundary on the Great Bank of Guizhou (Lehrmann et al., 2006).

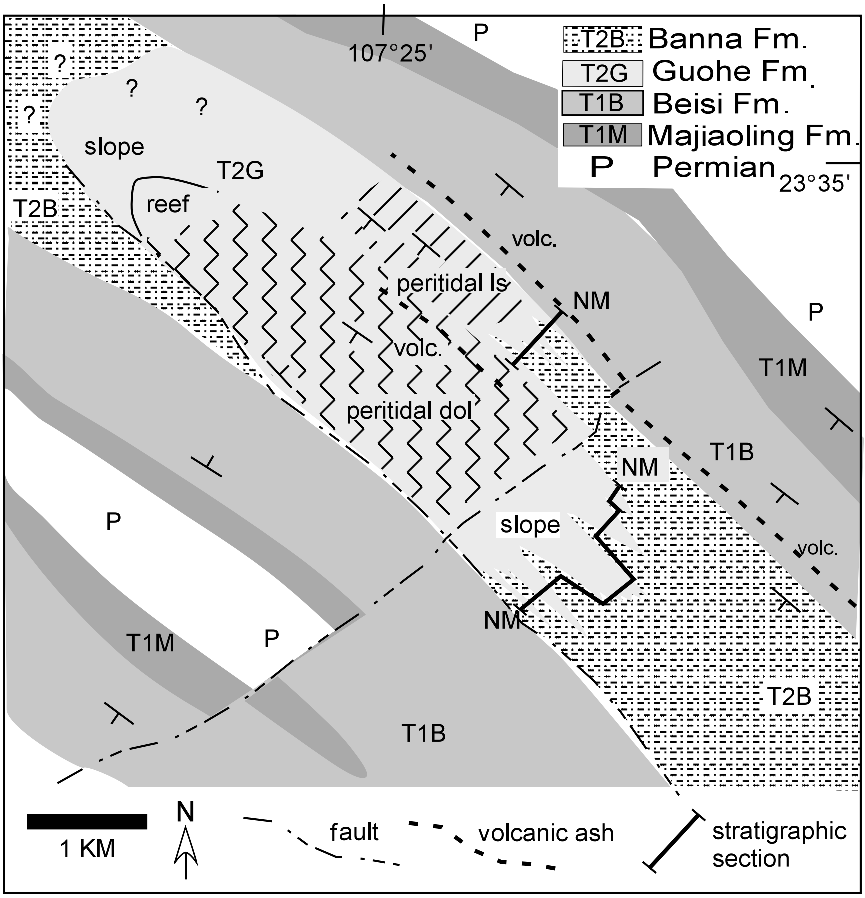

Figure 9. Detailed map of the northern pinnacle platform of the Pingguo area. The NM section is presented in Figure 11; the location is in Figure 8.

Banmo Limestone Member

The Banmo limestone member overlies the volcanic member (Figure 7). It consists of shallow-marine skeletal and oncolitic limestone that changes upward to deep-marine, dark-gray, nodular-bedded lime wackestones and laminated argillaceous lime mudstone, marking the drowning and siliciclastic burial of the western part of the CPP. Here, the lower part of the Banmo consists of rhythmic intercalation of dark-gray to pinkish-gray oncolitic skeletal packstone and argillaceous nodular lime mudstone and wackestone (Figure 7). The interval contains a diverse open-marine fauna (Table 2). Oncoids have irregular cauliflower shapes, typically nucleate on bivalve or crinoid fragments, and are encrusted by cyanobacteria and foraminifers (Figure 13A). The oncoids are interpreted to represent deeper water algal nodules occasionally turned during storms. Similar algal nodules have been found in the drowning sequence of other platforms in the Nanpanjiang Basin (Lehrmann et al., 1998) and have been found in deep-water slope environments of modern platforms (Enos and Perkins, 1977). The oncolite is overlain by darker nodular-bedded lime wackestone (Figures 7, 13B), followed by laminated argillaceous lime mudstones (Figure 13C) containing deep-marine fauna (Table 2). The succession is interpreted to represent drowning and termination of carbonate sedimentation in the Chongzuo area. Carbonates were buried by siliciclastics of the Banna Formation (Figure 7).

In the Pingguo area, the Banna Formation represents drowning of a large area of the platform as the interior was flooded and shallow-marine carbonate deposition backstepped to form smaller pinnacle platforms of the Guohua Formation (Figure 8). In this area, the lower part of the Banmo member consists of partly dolomitized carbonate mudstones and wackestones with restricted molluskan fauna that represent continued platform growth following the deposition of volcanic ash across the platform (Figure 10). The presence of several hardgrounds (Figures 11, 13D) reflects pauses in sediment accumulation. These are followed by black, nodular lime mudstones containing deep-marine fauna (Table 2). The succession provides relatively unambiguous evidence for termination of shallow-marine carbonate sedimentation by drowning. The Banmo member is interpreted to be Middle

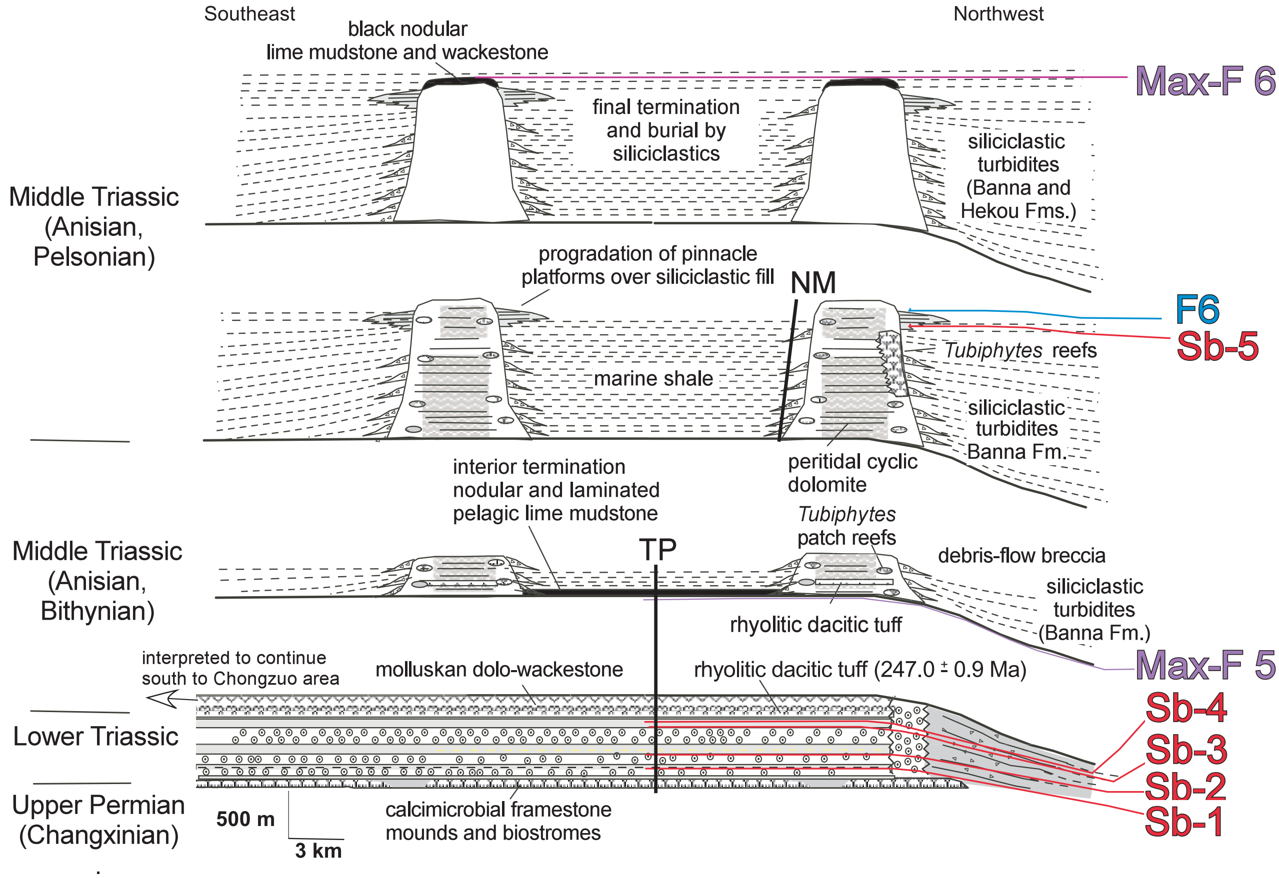

Figure 10. Restored cross sections of the CPP illustrating Late Permian to Middle Triassic evolution and sequence stratigraphy. Sections TP and NM are presented in Figure 11 (locations in Figures 8, 9). Sb = sequence boundary, F = flooding surface, Max-F = maximum flooding surface.

Triassic (Bithynian) in age on the basis of the foraminifers *Meandrospira* and *Pilammina*(?), the conodonts *C. gondolelloides* and *Neogondolella regalis*, and the ammonoids *Protrachyceras*, *Bulogites*, and *Paraceratites*. The Banmo member is overlain by the Banna siliciclastic member, a thick succession of shale and sandstone turbidites (Table 2; Figures 7, 11).

Middle Triassic Guohua Formation

The Guohua Formation consists of a complex of interior, reef-margin, and slope facies that form at least three isolated pinnacle platforms in the Pingguo area (Figures 4, 8). The pinnacle platforms range from 4 to 8 km (2.5 to 5 mi) across and have a thickness of 1700 m (5577 ft) measured at the NM section (Figures 8, 11). The isolated nature of the pinnacles is demonstrated by the pinch-out of the Banna siliciclastic member from the TP section to the northeast and southeast against the Guohua Formation (Figures 8, 9).

The facies distribution of the northern pinnacle is illustrated in Figure 9. The platform-interior facies is composed of thick-bedded, cyclic peritidal limestone and dolomite (Table 2; Figure 9). Massive *Tubiphytes* boundstone approximately 200 m (660 ft) thick occurs at the northern margin (Figure 9). The boundstone is composed of branching *Tubiphytes* frameworks, reinforced by encrusting fossils and marine cement (Table 2; Figure 14A). No in-place reefs were found on the southeast margin of the northern pinnacle (Figure 9), but the presence of *Tubiphytes* boundstone clasts in slope breccias at NM section (Figures 9, 11) indicates patch reefs, at least, developed along the southeast margin. In-place *Tubiphytes* patch reefs crop out on the northeast margin of the southerly pinnacle north of Pingguo (Figure 10).

Basin-margin facies flank the pinnacles. The best exposures, at the NM section, are composed of a series of intertonguing carbonate wedges and tongues of shale and turbidite sandstones (Figures 9, 14B). The carbonate intervals consist of black, laminated lime mudstone with slump folds punctuated by polymict debris-flow breccias (Table 2; Figure 14C, D). The lime mudstone contains pelagic fauna (Table 2). Breccias are dominantly clast supported, with pebble- to boulder-size clasts of *Tubiphytes* boundstone, *Tubiphytes*-fragment grainstone, oncolite-intraclastic packstone, molluskan wackestone and packstone, and black, tabular lime mudstone. This assortment indicates that erosion tapped into platform-interior, as well as platform-margin and slope, lithologies. The succession of conodonts from the NM section (*Nicoraella germanica* and *Nicoraella kockeli*, followed by *Neogondolella bulgarica*) indicates Bithynian and Pelsonian ages (Figure 11). Intertonguing relationships at the NM section demonstrates that the pinnacle platform grew synchronously with siliciclastic basin fill (Figure 10). A final stage of progradation of shallow-marine carbonates over basin-filling clastics is evident in the southern pinnacle platform and the northern margin of the pinnacle in the Guohua area defining sequence 5 (Figure 10).

The final termination of the Guohua Formation is preserved in the southern pinnacle, where the Guohua Formation is overlain by siliciclastics of the Banna Formation (north of Pingguo, Figures 8, 10). The termination is marked by a shift to black, nodular-bedded, oncolitic wackestone followed by shale, indicating termination by drowning. Conodonts within the drowning interval include *N. bulgarica*, a Pelsonian form. Termination of the Guohua pinnacles signifies the end of carbonate deposition in the Nanpanjiang Basin everywhere in Guangxi (Figure 5).

Heshan Platform

The Heshan platform, approximately 100 km (62 mi) east of Pingguo, is the second largest in the basin (Figure 3; Table 1). The extent of the platform is constrained, except to the east, by the distribution of Majiaoling, Beisi, and Loulou formations in regional maps (Figure 3).

The early evolution was similar to that of the CPP, but it lacks the volcanics and the Middle Triassic pinnacles (Figures 3, 4). The platform formed a low-relief bank during the Early Triassic, with shallow-marine, cyclic oolitic carbonates similar to the CPP. The platform was drowned and buried with basinal siliciclastics near the end of the Early Triassic (Table 1). The presence of the conodonts *Neospathodus triangularis*, *Neospathodus homeri*, and *Neospathodus symmetricus* indicates the termination of the Heshan platform in the Early Triassic (Spathian), substantially earlier than the early Anisian drowning of the CPP. The facies succession, including cherty, argillaceous, nodular-bedded lime wackestones, indicates termination by drowning. Kessel et al. (2002) noted the lighter color and greater argillaceous content of the nodular facies, however, suggesting a greater function of siliciclastic influx in platform termination compared with the CPP.

Debao Platform

The Debao platform, 100 km west of Pingguo, is the third largest (Figure 3). As in the Pingguo area of the CPP, the platform evolved as a low-relief bank with oolites in the Early Triassic and pinnacles with *Tubiphytes* reefs in the Middle Triassic (Table 1). Regional geologic maps record no Guohua Formation in this area to indicate the development of Middle Triassic pinnacle platforms (Figure 4). However, basinal sediments at Jingde (Figure 4) include allochthonous, debris-flow breccias containing *Tubiphytes*-boundstone clasts, indicating slope sedimentation proximal to Middle Triassic carbonate buildups bearing reefs.

Great Bank of Guizhou

The Great Bank of Guizhou is the smallest, northernmost, and longest lived platform in the basin (Figure 3; Table 1). The detailed facies architecture and evolution were presented by Lehrmann et al. (1998). The following summarizes the depositional history, sequence stratigraphy, and observations critical for comparison with other platforms in the basin.

In the latest Permian, the Great Bank of Guizhou nucleated on antecedent topography near the former margin of the Yangtze platform during a transgression that drowned shallow-marine carbonates in the surrounding area (Table 1). During the Early Triassic, the platform evolved as a low-relief bank with oolite margins, but substantially thinner than coeval platforms in the southern part of the basin (Figure 15; Table 1). Four depositional sequences are represented by platform-interior facies–stacking patterns and basin-margin facies shifts. Sequence 1 is defined in the platform interior as an upward change from thin-bedded lime mudstone to cross-bedded ooid dolograinstone and cryptalgal laminite dolostone (Figure 15, SB-1). This was followed by flooding and shift to deeper subtidal carbonates at the base of the peritidal cyclic limestone facies (Figure 15, F-2). At least two depositional sequences are recorded in the peritidal cyclic limestone facies by parasequence stacking patterns (Figure 15, SB-2, 3; Lehrmann et al.,

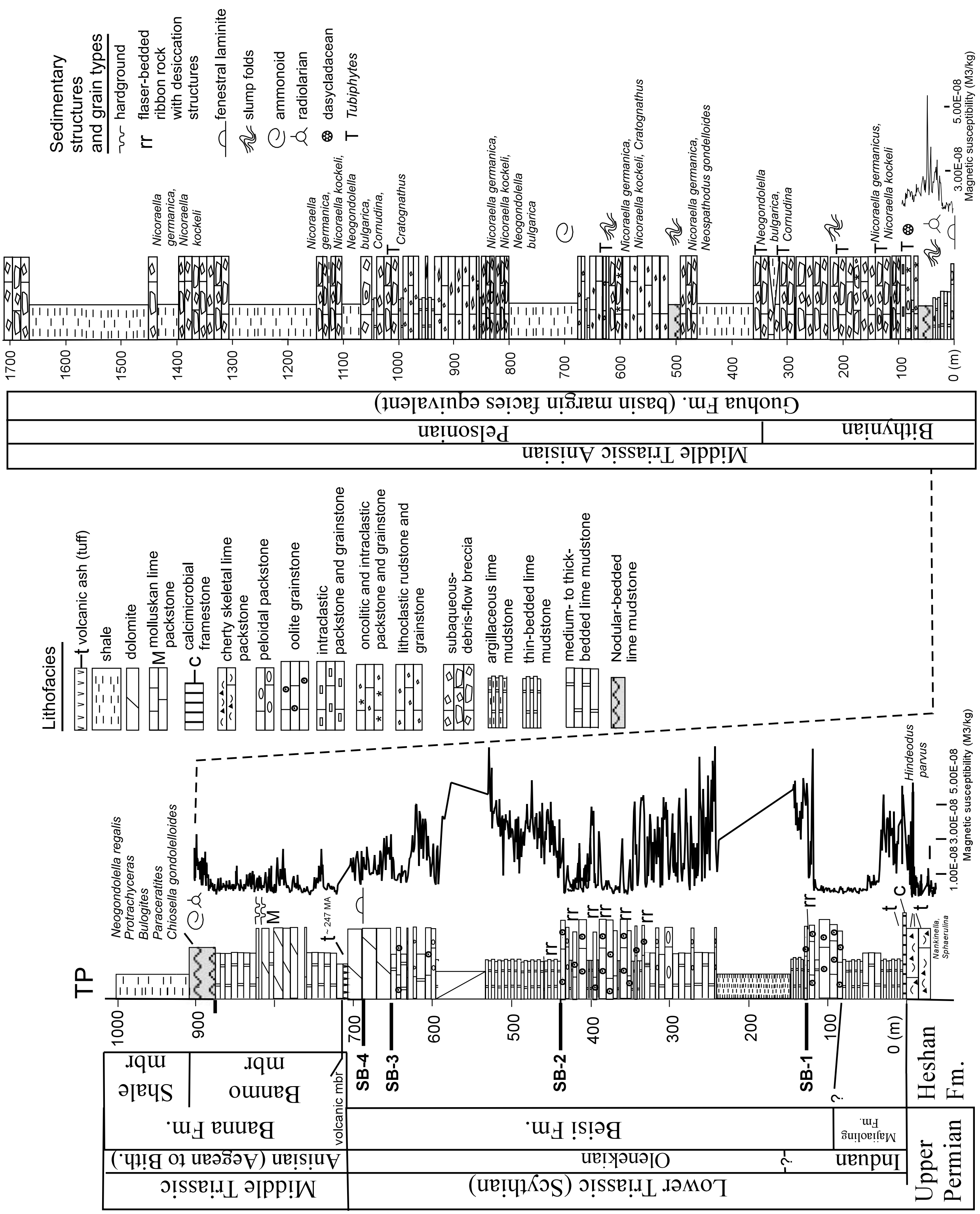

TP
NM
Middle Triassic
Anisian (Aegean to Bith.)
Lower Triassic (Scythian)
Olenekian
Indian
Upper Permian
Banna Fm.
Shale mbr
Banmo mbr
volcanic mbr
Beisi Fm.
Majiaoling Fm.
Heshan Fm.
SB-4
SB-3
SB-2
SB-1
Middle Triassic Anisian
Pelsonian
Bithynian
Guohua Fm. (basin margin facies equivalent)
Neogondolella regalis
Protrachyceras
Bulogites
Paraceratites
Chiosella gondolelloides
t ~247 MA
Hindeodus parvus
Nankinella, Sphaerulina
1.00E-08 3.00E-08 5.00E-08
Magnetic susceptibility (M3/kg)
Lithofacies
volcanic ash (tuff)
shale
dolomite
molluskan lime packstone
calcimicrobial framestone
cherty skeletal lime packstone
peloidal packstone
oolite grainstone
intraclastic packstone and grainstone
oncolitic and intraclastic packstone and grainstone
lithoclastic rudstone and grainstone
subaqueous-debris-flow breccia
argillaceous lime mudstone
thin-bedded lime mudstone
medium- to thick-bedded lime mudstone
Nodular-bedded lime mudstone
Sedimentary structures and grain types
hardground
flaser-bedded ribbon rock with desiccation structures
fenestral laminite
slump folds
ammonoid
radiolarian
dasycladacean
Tubiphytes
Nicoraella germanica, Nicoraella kockeli
Nicoraella germanica, Nicoraella kockeli, Neogondolella bulgarica, Cornudina, Cratognathus
Nicoraella germanica, Nicoraella kockeli, Neogondolella bulgarica
Nicoraella germanica, Nicoraella kockeli, Cratognathus
Nicoraella germanica, Neospathodus gondelloides
Neogondolella bulgarica, Cornudina
Nicoraella germanicus, Nicoraella kockeli
3.00E-08 5.00E-08
Magnetic susceptibility (M3/kg)

2001). Finally, a fourth depositional sequence is recorded near the top of the Lower Triassic by a dramatic shift to a thick interval of dolomitized debris-flow breccias at the basin margin (Figure 15, SB-4).

Volcanic-ash deposits on the north flank of the Great Bank of Guizhou (Figure 15) are biostratigraphically the same age as the volcanics from the CPP in the southern part of the basin and yield similar radiometric ages (Lehrmann et al., 2006, unpublished data). In contrast to the CPP, however, the volcanic units are thin and occur only in the basin margin.

Tubiphytes reefs grew at the platform margin as the platform developed a flat-topped, progressively steepening profile during the Anisian (Figure 15; Table 1). Platform-margin geometries demonstrate the development of 400 m (1300 ft) of platform relief over the adjacent basin margin, and slope angles steepened up to 30° by the end of the Anisian. Progradation of the platform was followed by aggradation, erosional retreat of the reef margin, and finally, prolonged exposure in the platform interior as indicated by amalgamated tepee complexes capping depositional sequence 5 (Figure 15, SB-5). Although 600–750 m (1968–2460 ft) of carbonate accumulation in the Great Bank of Guizhou during the Anisian is impressive, it is far thinner than the 1700 m (5577 ft) of accumulation in the pinnacles of the CPP during the Bithynian and Pelsonian, roughly half of the Anisian (Figure 10; Table 1).

During the Ladinian, the Great Bank of Guizhou developed a high-relief escarpment, with approximately 1900 m (6233 ft) of relief above the adjacent basin margin (Figure 15). The platform interior shifted from a flat-topped profile to an atoll-like profile with a submerged lagoon, and eventually back to a flat-topped profile, with tidal flats extending across the platform (Figure 15). Depositional sequences are defined by a shallowing and shift to peritidal facies above the reef complex (Figure 15, SB-6), followed by flooding and initiation of the interior lagoon (Figure 15, F-7), and subsequent restoration of a flat-topped profile with tepee complexes as evidence of prolonged exposure (Figure 15, SB-7). Following SB-7, the platform interior was again flooded, resulting in subtidal peloidal carbonates (Figure 15, F-8). Continued deepening resulted in the deposition of nodular, pelagic carbonates with deep-marine conodonts and marine-reptile fragments as the platform drowned during the Carnian (Figure 15, Max-F 8). Drowning of the platform preceded burial by siliciclastics in the Carnian (Figure 15).

CONTROLS ON PLATFORM EVOLUTION

Tectonic Subsidence

Subsidence analyses were performed in eight areas including four sites on the Yangtze platform, two sites on the CPP, another on the Great Bank of Guizhou, and one, Huishui, in the basin center (Figure 3). Only two of the areas, Luocheng and Guiyang, in the Yangtze platform expose the section down to the Proterozoic basement. The oldest strata exposed in the other six subareas range from Devonian to Ordovician.

The Proterozoic to Triassic subsidence pattern in the Guiyang area (Figure 16A) is generally representative of the Yangtze platform. The long-term patterns of subsidence are consistent with the tectonic history of the South China block interpreted from previous studies (see the section on geologic setting). Slow subsidence accompanied cratonic sedimentation in the Proterozoic following the stabilization of the South China craton (Figure 16). The early Paleozoic subsidence profile (530–450 Ma) exhibits decelerating subsidence signifying thermal subsidence of a passive margin (Figure 16A-1). Mean tectonic-subsidence rates, omitting extreme values influenced by abnormally thick strata or short time frames, of 21 m/m.y. (68 ft/m.y.) during the Cambrian followed by 2.5 m/m.y. (8.2 ft/m.y.) in the Ordovician are consistent with passive-margin development (cf. Bond and Kominz, 1984). Uplift during the Devonian, followed again by exponential decay in subsidence rates (up to 42 m/m.y. [137 ft/m.y.] in the Devonian; average 3.4 m/m.y. [11.1 ft/m.y.] in the Carboniferous), is consistent with rifting and passive-margin development as the South China plate separated from Gondwana during the Guangxi orogeny (Figure 16A-2). Renewed uplift and subsequent subsidence in the Late Permian is consistent with extension during the Dongwu movement (Figure 16A-3). Finally, accelerating subsidence

Figure 11. Stratigraphic sections from the Pingguo area. The TP section is of Permian to basal Middle Triassic strata of the platform interior. The NM section is in the Middle Triassic basin-margin facies south of the northern pinnacle platform. See Figures 8–10 for section locations. Dashed line shows correlation of termination of platform carbonates at the top of the Banmo member of the Banna Formation. The termination is near the top of the TP section and the base of the NM section. Note the change in scale between sections.

Table 2. Facies and Depositional Environments of the CPP

Age	Formation	Description	Fossils	Thickness	Depositional Environments
Middle Triassic	Siliciclastic member of Banna Fm.	Shale, mudrock punctuated by interbeds of sandstone. Bouma sequences.	Thin-shelled bivalves, ammonoids.	>1500 m; >4921 ft	Hemipelagic mud and turbidites.
Middle Triassic (Bithynian–Pelsonian)	Guohua Fm.	Peritidal cyclic limestone and dolomite with intraclastic, oncolitic, domal stromatolites bioturbated skeletal packstone bases, fenestral-laminate caps. *Tubiphytes* boundstone. Debris-flow breccias intertonguing with lime mudstone (nodular-bedded, horizontally laminated) and shale.	Bivalves, gastropods, dasycladaceans, foraminifers, *Tubiphytes, Baccinela* spongiostromate algae, ammonoids. Radiolarians, and conodonts.	1700 m; 5577 ft	Peritidal, restricted interior, margin reefs and deep-marine basin-margin slope.
Middle Triassic (early Bithynian)	Banmo member of Banna Fm.	Lower: skeletal and oncolitic lime packstone-grainstone alternating with lime mudstone in Chongzhuo. Dolostone with hardgrounds in Pingguo. Upper: Dark nodular bedded lime mudstone and laminated argillaceous limestone in upper part.	Bivalves, gastropods, ostracods, crinoids, foraminifers, dasycladacean algae. Ammonoids and conodonts in upper part.	200–327 m; 660–1072 ft	Shallow-subtidal restricted to open-marine lower part; deep-marine drowned platform upper part.
Early–Middle Triassic (Olenekian–Anisian) boundary	Volcanic member of Banna Fm.	Porphyritic rhyolite and rhyolitic dacite-dacite pyroclastic breccias and tuff. Coherent facies (lava flows) with euhedral crystals, plagioclase microlites, and spherulites lacking glass shards or shattered phenocrysts. Pyroclastic facies with glass shards, shattered crystals.	500 to >1640 m (1640 to >5380 ft) reported in Chongzou area by Guangxi Bureau; 6 m (19 ft) in Pingguo area.		Subaerial and subaqueous ash fall and rhyolite lava flows.
Early Triassic	Luolou Fm.	Thin-bedded, dark gray-black, laminated to horizontally burrowed, pyritic lime mudstone. Shale intercalations and polymict debris-flow breccias. Slump folds. Clast-supported breccias, pebble to cobble sized, rounded to angular clasts of oolite packstone and grainstone, and black, tabular lime mudstone.	Thin-shelled bivalves, ammonites, foraminifers, and conodonts.	40–530 m; 131–1738 ft	Deep-marine basin and slope. Mostly anoxic.
Early–Middle Triassic (Olenekian–basal Bithynian)	Beisi Fm.	Thin-bedded, light-gray lime mudstone, wavy laminated with few burrows, argillaceous partings between beds. Massive to cross-bedded oolite grainstone. Ribbon rock, fenestral fabric and desiccation cracks. Dolostone in upper part.	Bivalves, thin-shelled pectinoid bivalves, gastropods, ostracods, foraminifers.	630–802 m; 2066–2361 ft	Restricted marine. Sequences shallow from subtidal to high-energy intertidal and supratidal.

Early Triassic Induan	Majiaoling Fm.	Thin (2–10 cm; 0.8–4 in.) flaggy, homogeneous beds of light- to medium-gray lime mudstone and argillaceous lime mudstone with argillaceous partings. Wavy lamination or vague burrows. Thin oolite stringers in fining-up beds with scoured bases. Thicker bedding (0.5–1 m; 1.6–3.3 ft) in basal part in Chongzuo area.	Rare gastropods, bivalves, and foraminifers.	90–100 m; 295–330 ft	Marine subtidal between normal and storm-wave base. Restricted? Storm beds.
Earliest Triassic	Basal Majiaoling Fm.	Calcimicrobial biostromes with wavy, vaguely mounded beds and discrete domes up to 1 m (3.3 ft) thick. Globular micrite-walled chambered fossils form framework surrounding irregular internal cavities.	Calcified coccoid cyanobacteria, bivalves, gastropods, ostracods, foraminifers, echinoderms.	5 m; 16 ft	Shallow subtidal, open marine.
Late Permian	Dalong Fm.	Dark-gray spiculitic mudrock, chert, and cherty argillaceous limestone.	Ammonoids, bivalves, radiolarians, small articulate brachiopods.	up to 160 m (524 ft)	Open marine, Deep water.
Late Permian	Upper Heshan Fm.	Medium-gray to black, cherty, skeletal lime packstone and minor grainstone. Massive beds 0.5–1 m (1.6–3.3 ft) thick. Chert nodules. Fragmented fossils. Infiltrated sediments with perched fabrics. Several subaqueous volcanic-ash layers 0.1–0.5 m (0.3–1.6 ft) thick.	Articulate brachiopods, bryozoans, foraminifers fusulinids, crinoids, bivalves, gastropods, dasycladacean algae.	225 m; 738 ft	Shallow subtidal, open marine. Occasionally winnowed.

rates in the Triassic are consistent with foreland-basin development during the Indosinian orogeny (cf. Allen et al., 1986) (Figure 16A-4).

Because basement rocks are not exposed in the remaining subareas of the basin, plots for these areas begin above the basinwide unconformity developed in the Middle Devonian (Figure 16B–D). Although subsidence profiles are typically built from the basement, we believe this approach is acceptable because the Middle Devonian unconformity represents a major basin reorganization and a renewed subsidence following basinwide emergence and erosion. A consistent pattern of exponential decay in subsidence beginning in the Devonian, followed by Late Permian uplift and accelerating Triassic subsidence that developed in all subareas of the basin, gives us confidence that these patterns are driven by basin tectonics.

The inflection point at the onset of the Indosinian orogeny occurs at the beginning of the Triassic or beginning of the Olenekian (Figure 16), indicating that foreland-basin development was initiated in the Triassic. Accelerating subsidence and rates greater than 350 m/m.y. (1148 ft/m.y.) are consistent with foreland-basin models (Allen et al., 1986). The accelerating subsidence pattern may have been produced by either (1) thrust loading and flexural subsidence of the lithosphere, accompanied by progressive cratonward migration of the foredeep depozone; or (2) dynamic topography associated with subduction (Gurnis, 1992) or a combination thereof. Among the isolated carbonate platforms, peak subsidence rates occurred earlier in the southern part of the basin (Olenekian, Pingguo, and Chongzuo areas; Figure 16C, D) than in the northern part of the basin (Carnian, Great Bank of Guizhou, Figure 16B). Although the peak subsidence of the Yangtze platform appears to have occurred during the Olenekian in the Guiyang area (Figure 16A), in the western sector (Zhenfang, Guanling; Figure 4), peak subsidence up to 290 m/m.y. (951 ft/m.y.) was reached in the Carnian as the platform drowned and was buried by siliciclastic turbidites (Enos et al., 1998; Koenig et al., 2001).

Comparison of carbonate-platform architecture with the subsidence curves demonstrates a strong tectonic control on overall platform architecture and history. Platforms in the southern part of the basin (CPP, Heshan, and Debao) were drowned and buried by clastics earlier, during the end of the Early Triassic or beginning of the Middle Triassic, in response to greater subsidence and earlier peak rates in the southern part of the basin (Figures 3–5, 16). Platforms in the northern part of the basin (Great Bank of Guizhou, Yangtze

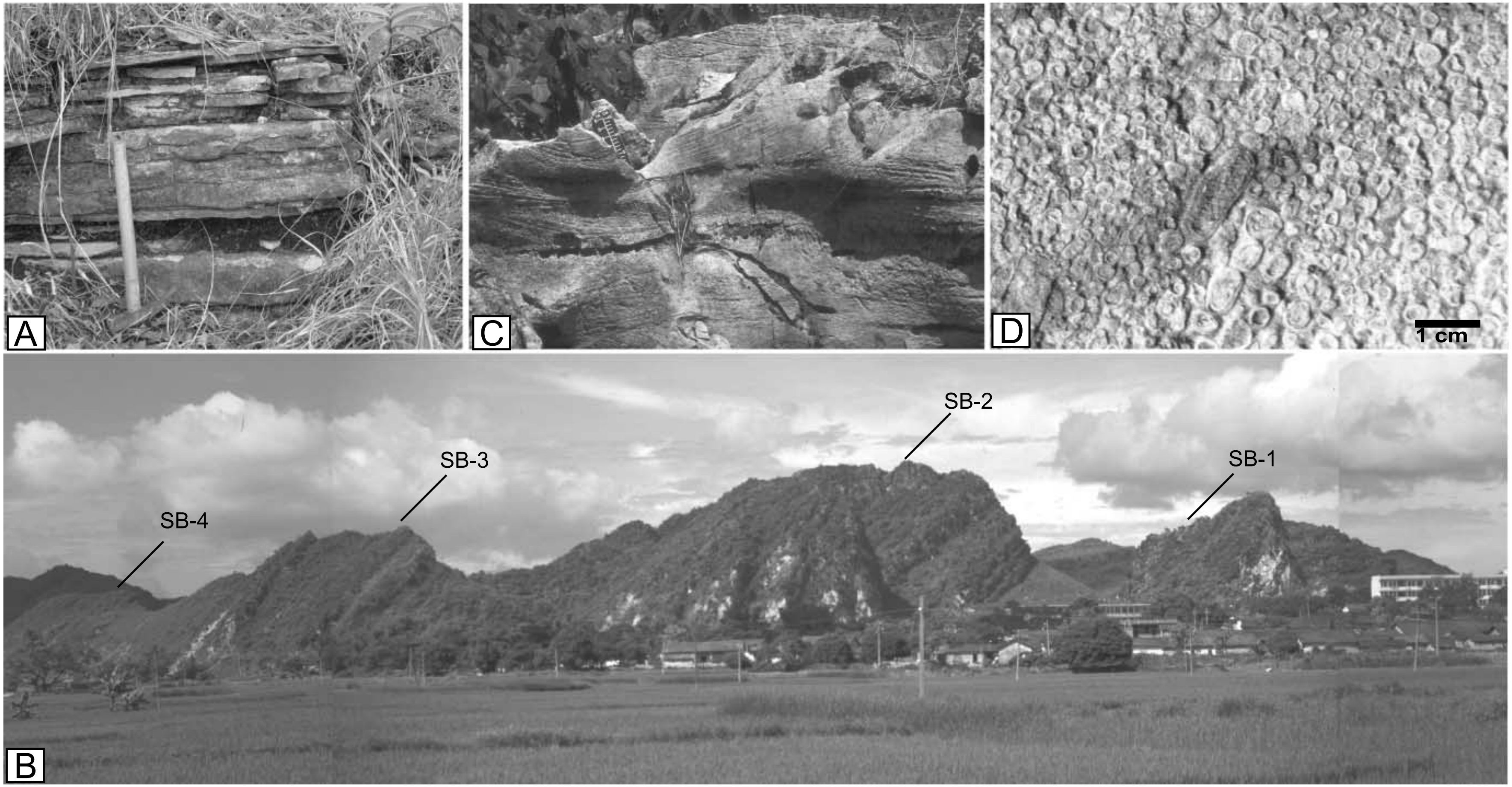

Figure 12. Lower Triassic platform interior facies of the CPP; Majiaoling and Beisi formations. (A) Flaggy, thin-bedded lime mudstone typical of the Majiaoling Formation, LY section, 78 m (255 ft). (B) Majiaoling and Beisi formations at the LY section, Chongzuo area (Figures 6, 7) Cliff-forming units are oolite; recessive intervals contain greater parts of lime mudstone. Strata are arranged into four sequences with oolite in upper parts (SB-1 to SB-4). (C) Cross-bedded oolite of the Beisi Formation, LY section. Scale bar is 15 cm (6 in.). (D) Oolite grainstone of the Beisi Formation (northern platform margin, Pingguo area). Note giant ooids up to 1 cm (0.4 in.) across (center).

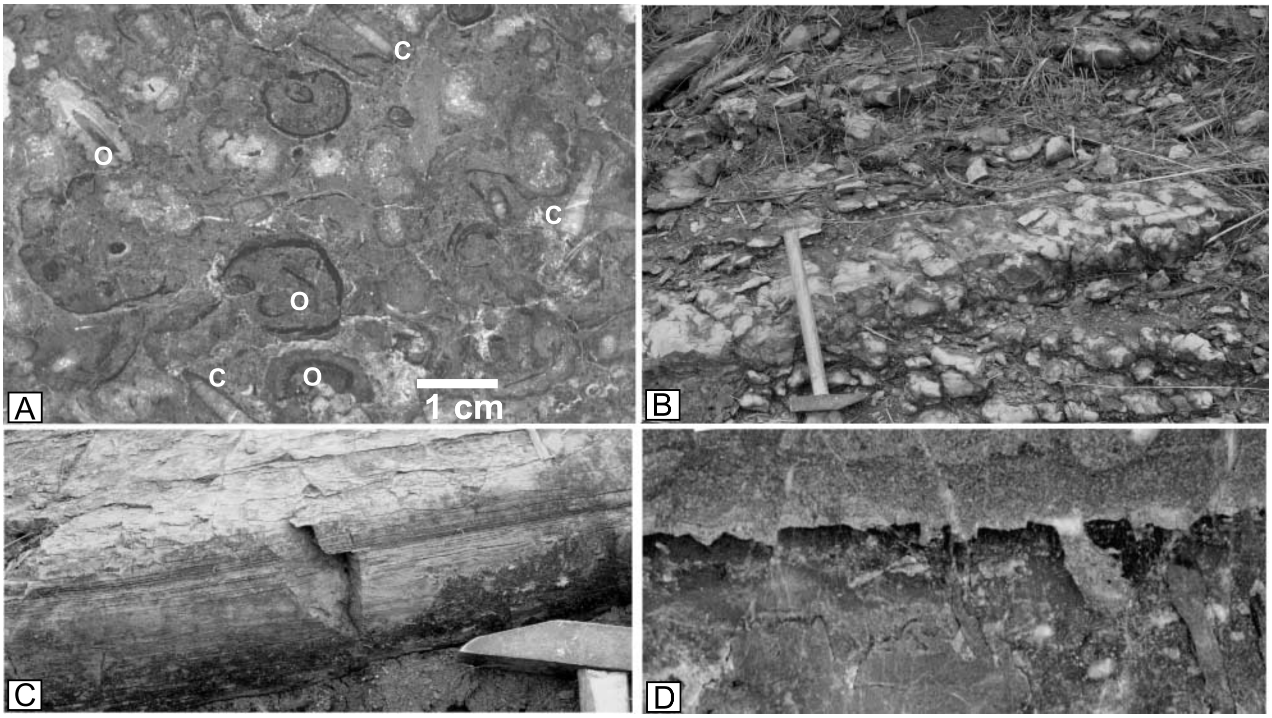

Figure 13. Middle Triassic Aegean–Bithynian facies of the Banmo member of the Banna Formation of the CPP. (A) Polished slab of oncolitic lime packstone from the lower Banmo member. Note crinoids (C) and oncoids (O). Oncoids commonly have pustular morphology (upper left). Nearly all grains have coatings of cyanobacteria, foraminifers, and unidentified skeletal encrusters. From the BM section, 278 m (912 ft). Chongzuo area (Figure 7). (B) Black, nodular-bedded lime wackestone of the upper Banmo member (drowning succession) at the BM section, 475 m (1558 ft). (C) Laminated argillaceous lime mudstone of the upper Banmo member (drowning succession) at the BM section, 311 m (1020 ft). (D) Polished slab of hardground in the lower Banmo member at TP section, 820 m (2690 ft) (Figure 11).

platform) were drowned and buried in response to later (Carnian) peak subsidence.

High subsidence rates during the Olenekian and Anisian resulted in extremely thick Lower Triassic carbonates (Beisi Formation) across the CPP and backstep and pinnacle morphology in the Pingguo area (Guohua Formation). Progressively increasing subsidence contributed to the progressive steepening megabank architecture of the Great Bank of Guizhou, the evolution from bank to rimmed platform to high-relief-escarpment profile. Lower rates of subsidence in the Guiyang area of the Yangtze platform resulted in Ladinian progradation (Enos et al., 1998; Koenig et al., 2001), in stark contrast to the morphology of the isolated platforms. Finally, high rates of subsidence contributed to the drowning of the western sector of the Yangtze platform during the Carnian, whereas lesser rates maintained platform sedimentation in the Guiyang area (Enos et al., 1998).

The coincidence of drowning with peak subsidence rates demonstrates that tectonic subsidence can drown carbonate platforms without other mechanisms such as eustatic sea level rise, siliciclastic influx, or upwelling of cool, nutrient-rich waters. Termination horizons in the CPP, Heshan, Debao, and the Great Bank of Guizhou platforms lack evidence of phosphates or greatly increased bioerosion that would indicate influx of excess nutrients (Hallock and Schlager, 1986). Although progressive northward movement of the South China plate would be an appealing mechanism for the termination of carbonate sedimentation by cooling climate, paleomagnetic data indicate a position well within the tropics during termination, and the northernmost platforms (Great Bank of Guizhou, Yangtze platform) were the last to perish. Moreover, carbonate facies lack evidence of a shift to cool-water, heterozoan fauna (James, 1997). Platform facies continue to contain tropical carbonate associations of lime mud and oolite until just prior to platform termination. In the termination sequence of the Great Bank of Guizhou, for example, tropical carbonates, including oolite and scleractinian corals, occur immediately beneath the termination horizon (Lehrmann et al., 1998).

Peak subsidence rates of 400 m/m.y. (1312 ft/m.y.) drowned most of the platform areas in the southern

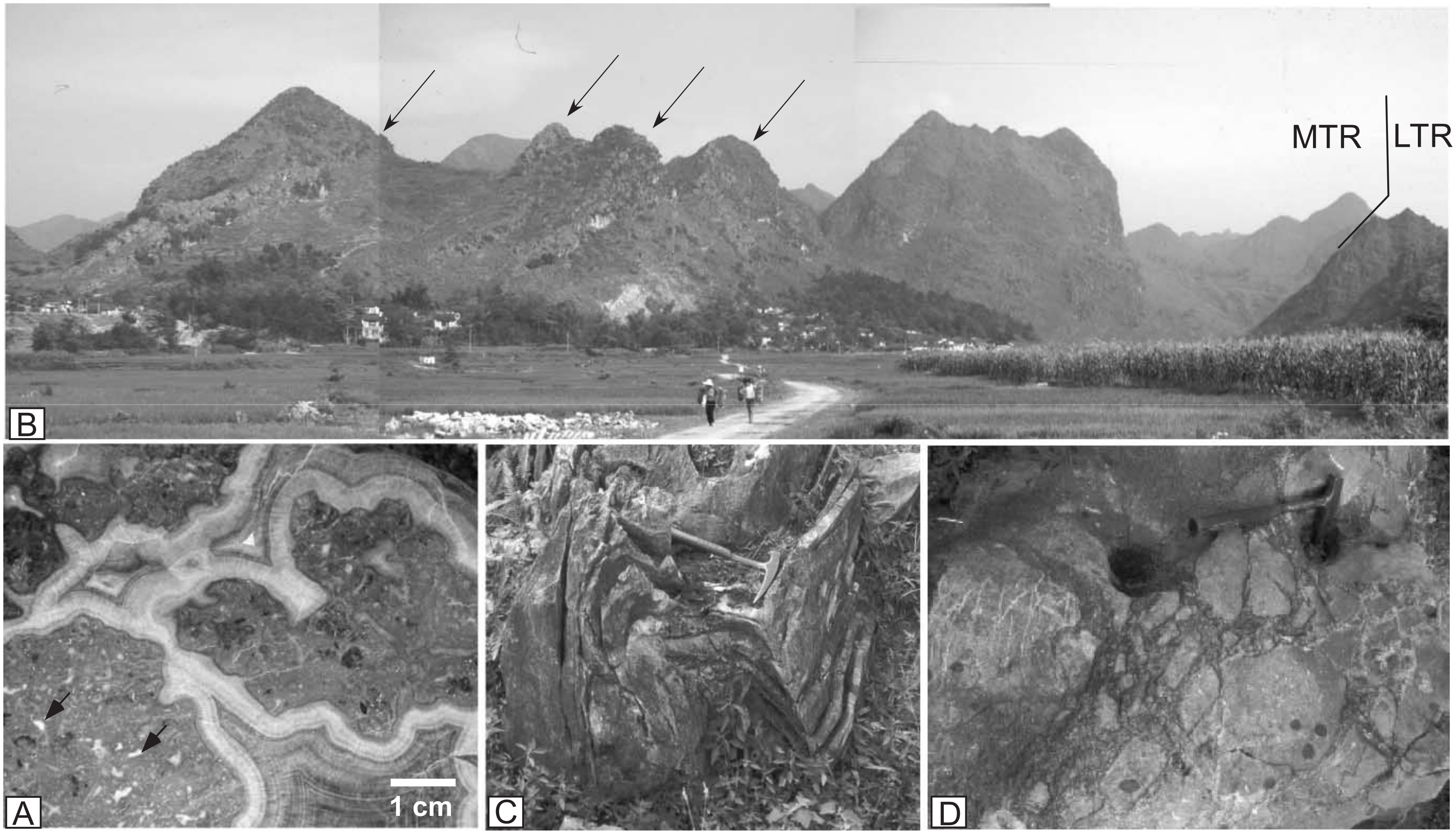

Figure 14. Middle Triassic facies of the Guohua Formation pinnacle platform in the Pingguo area (Figures 4, 9, 10). (A) Polished slab of *Tubiphytes* boundstone from reef facies along the northern margin of the northern Pingguo pinnacle. *Tubiphytes* are small, branching, framework-building fossils (arrows). Note that most of this rock is composed of isopachous marine cement. (B) Field photo of basin-margin succession flanking the southern margin of the Pingguo pinnacle at the NM section (Figure 9). Photo view toward the northwest along depositional strike. Stratigraphic top is to the left. Lower Triassic strata at the far right are uppermost carbonates of the low-relief-bank phase of platform development (top of Beisi Formation). The recessive area in the foreground is composed of siliciclastic turbidites of the Banna Formation that intertongue with basin-margin carbonate breccias shed from the pinnacle platform (resistant ledges in photo). Arrows (parallel to dip of beds) indicate prominent tongues of carbonate debris-flow breccias. (C) Thin-bedded lime mudstone with slump folds; basin-margin succession, NM section, 620 m (2034 ft). (D) Polymict debris-flow breccia with large equant clasts of lime grainstone and *Tubiphytes* boundstone derived from the platform and smaller tabular clasts of lime mudstone derived from the slope. Basin-margin succession, NM section, 1110 m (3641 ft). MTR = Middle Triassic; LTR = Lower Triassic.

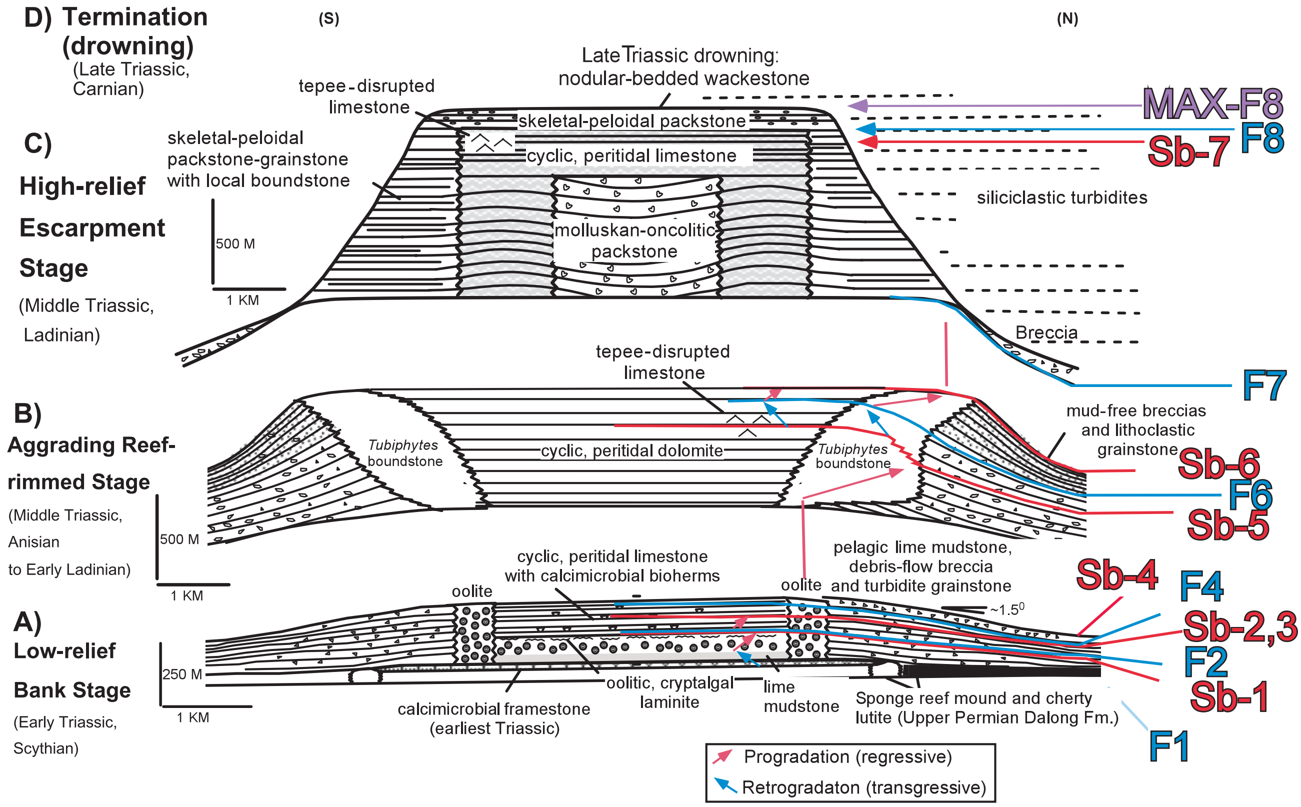

Figure 15. Restored cross sections of the Great Bank of Guizhou illustrating Late Permian to Late Triassic evolution. Cross section is from the northwest-trending syncline that dissects the platform (Figure 3 for location). For stratigraphic data, see Lehrmann et al. (1998). (A) Lower Triassic: low-relief bank stage; (B) Anisian–early Ladinian: aggrading reef-rimmed stage. (C) Ladinian: high-relief escarpment stage. (D) Carnian: termination (drowning). Sb = sequence boundary; F = flooding surface; Max-F = maximum flooding surface.

basin (CPP, Heshan, Debao) during the early Anisian. Drowning of the pinnacles in the Pingguo area was likewise driven by high subsidence rates in the Anisian. Finally, the Carnian drowning of the Great Bank of Guizhou also correlates with peak subsidence rates (Figure 16B). Schlager (1999) presented arguments to resolve his paradox of drowned carbonate platforms: that drowned platforms are common despite the fact that Holocene carbonate growth rates far exceed rates of tectonic subsidence and sea level rise. He demonstrated that carbonate growth rates decrease over longer periods through a regression of thickness with time for platform accumulation rates (Schlager et al., 1998) and through contrasting growth rates of prograding versus drowned platforms in the rock record (Schlager, 1999). These analyses yield an estimate of sustainable platform growth rates of 40 m/m.y. (131 ft/m.y.) at 100 Ma. Drowning episodes in the Nanpanjiang Basin occurred at times of peak subsidence, exceeding 200–350 m/m.y. (660–1148 ft/m.y.); this is consistent with drowning driven by tectonic subsidence (Figure 16). However, the Great Bank of Guizhou actively aggraded in the Early and Middle Triassic during subsidence at rates of 90–130 m/m.y. (295–426 ft/m.y.), and the CPP pinnacles prospered into the Anisian despite subsidence greater than 350 m/m.y. (1150 ft/m.y.), far exceeding the growth-potential estimate of Schlager (1999).

Volcanism

Volcanism had a significant impact on carbonate-platform evolution only proximal to the volcanic center. In the Chongzuo area, the thick pile of volcanics in the Banna Formation, up to 1640 m (5380 ft) thick, interrupted carbonate sedimentation and buried the platform in the early Anisian. Carbonate sedimentation resumed following the volcanism in the southwestern part of CPP, although a healthy, shallow-marine platform was never reestablished (Figure 7). The oncolitic skeletal packstone and argillaceous lime mudstone and wackestone

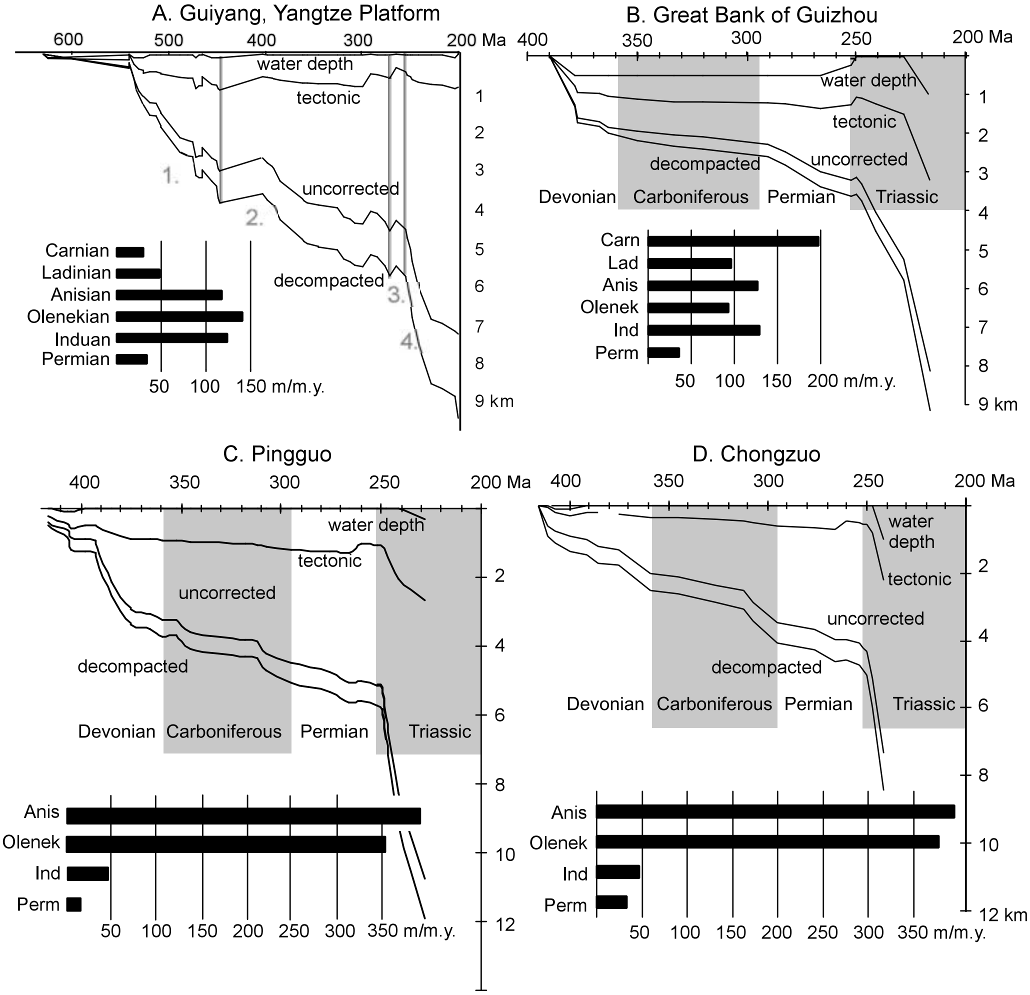

Figure 16. Subsidence histories for Yangtze platform (A) and Nanpanjiang Basin (B–D). Details of data compilation and back-stripping methods are presented in the methods section. (A) Proterozoic to Triassic subsidence history from the Yangtze platform margin in Guiyang (see Figure 3 for location). Interpreted tectonic events indicated numerically: (1) Early Paleozoic passive-margin development; (2) Guangxi orogeny, Devonian rifting of South China block from Gondwana; (3) Dongwu movement, Late Permian extension associated with Emeishan volcanism; (4) Indosinian orogeny, Triassic accelerating subsidence caused by foreland-basin development. (B) Devonian to Triassic subsidence history from the Great Bank of Guizhou. (C) Devonian to Triassic subsidence history from CPP in the Pingguo area. (D) Devonian to Triassic subsidence history from CPP in the Chongzuo area. Histograms show subsidence rates, using decompacted sediment thicknesses by stage for each area.

of the Banmo member represent a resurgence of carbonate sedimentation (Figure 7). The relatively thin accumulation, dark color, argillaceous content, and lack of restricted carbonate or shoal facies of the oncolite are interpreted to reflect relatively deep-marine accumulation. Overlying deposits are black, nodular carbonates, laminated argillaceous lime mudstone, and finally, siliciclastics, representing drowning of the platform. This succession indicates that subsidence submerged the platform following volcanism. Carbonate sedimentation resumed briefly following the volcanism but was unable to reestablish active platform growth as high rates of subsidence drowned the platform. We found no evidence that carbonate sedimentation resumed in the southeastern part of the platform around Chongzuo City, although the Guangxi Bureau of Geology and Mineral Resources (1985) has reported some fossiliferous shale and minor limestone within the volcanics. Very thick Banna volcanics are everywhere unconformably overlain by continental Lower Jurassic rocks. Thus, volcanism, and the thermal uplift associated with it, may have elevated the platform above sea level with a sheer volume of up to 1640 m (5380 ft) (Guangxi Bureau of Geology and Mineral Resources, 1985). The loading of the thick pile of volcanics may have contributed to subsidence, which subsequently drowned the platform.

In the central and northern part of the basin, volcanism had virtually no effect on platform evolution. Early Anisian volcanics apparently interrupted carbonate platform growth only briefly, depositing a layer 6 m (19 ft) thick that blankets the platform in the Pingguo area. Restricted, shallow-marine carbonate sedimentation prevailed prior to and following the volcanic episode, indicating that volcanism caused no significant change in platform sedimentation. In the Great Bank of Guizhou, volcanic horizons occur only in the basin-margin succession. Volcanic ash was probably eroded by wave and current action from the top of the platform.

Siliciclastic Influx

The impact of siliciclastic-sediment influx on carbonate depositional systems and the dynamics of mixed carbonate-clastic systems has been discussed in numerous articles. Isolated platforms of the Nanpanjiang Basin were essentially pure carbonate systems lacking siliciclastic deposition on bank tops. The timing of siliciclastic shale and turbidite fill in the basin, however, had a profound impact on platform evolution through a modification of slope geometry of the platform margins.

The lack of significant siliciclastic turbidite fill in the basin adjacent to the Great Bank of Guizhou during the Early and Middle Triassic led to a progressive steepening of basin-margin slopes (up to 30°), to retardation of basinward progradation, and eventually to a high-relief escarpment profile as subsidence and increasing water depths locked the platform into aggradational mode (Figure 15). In the absence of basin-filling siliciclastics, carbonate production was inadequate to fill the increasing accommodation space at the basin margin. The platform was finally buried by siliciclastics after it drowned during the Carnian (Figure 15). In contrast, earlier arrival of siliciclastics on the CPP resulted in burial of much of the platform following drowning in the early Anisian and in lower slope angles on the pinnacles in the Pingguo area (Figure 10). The pinnacles grew upward, concurrent with siliciclastic turbidite fill at the basin margin as evidenced by the intertonguing of slope carbonates and basinal turbidites. The fill of the basin prevented a progressive steepening of the slope and the development of a high relief above the basin floor as the pinnacles aggraded. Finally, the late-stage progradation of the pinnacles was facilitated by turbidite fill at the basin margin (Figure 10, SB-5).

Facies successions and subsidence histories indicate that platforms were terminated primarily by drowning in response to high subsidence rates. Siliciclastic influx, however, may have contributed to the termination of the Heshan platform as suggested by the lighter color and greater argillaceous content of nodular-bedded carbonates at the top of the platform and the early termination of the Heshan platform compared with the CPP.

The timing and source areas of turbidite fill in the Nanpanjiang Basin are poorly understood. The earlier turbidite fill (early Anisian) and burial of platforms in the southern basin and later arrival of siliciclastics in the northern basin (Ladinian and Carnian) are consistent with a southerly source area, probably an uplifted thrust belt to the south of a foreland basin (Figures 3–5). Zhang (1986) interpreted flow directions from the south for the Middle Triassic basin fill in Guangxi, and Wu and Li (1993, p. 132) showed northwesterly paleocurrents from the Banna Formation in the western Guangxi (Xilin area, Figure 3). However, paleocurrents in turbidites of Ladinian and Carnian age in the northern part of the basin, adjacent to the Great Bank of Guizhou, and in the Zhenfeng area of the Yangtze platform (Figure 5) indicate transport from east to west (Sun et al., 1989; Chaikin, 2004; Enos et al., in press). Chaikin (2004) and Enos et al. (in press) interpreted the eastern sourcing of the turbidites from the Jiangnan uplift (Figure 5). An alternative possibility is that the source area lies to the south, and that currents were deflected westward by the basin configuration adjacent to the Great Bank of Guizhou.

Eustasy

Sea level changes are reflected in depositional sequences represented both by platform-margin geometries and platform-interior cycle-stacking patterns (cf. Goldhammer et al., 1993; Loucks and Sarg, 1993). Sequences 1–4 in the CPP are represented by major shallowing-upward packages capped with oolite and are correlated between the Chongzuo and Pingguo areas with magnetic susceptibility profiles (Figures 7, 11). The first three sequences correlate reasonably with platform-interior stacking in the Great Bank of Guizhou (Figure 15). The fourth sequence boundary (SB-4) is tentatively correlated with the deposition of a thick interval of breccia shed to the basin margin adjacent to the Great Bank of Guizhou (Figure 15). The correlation is supported by the occurrence of SB-4 below the basal Anisian volcanic horizon in both areas. Sequence 5, represented by middle

Anisian progradation of the Pingguo pinnacles (Figure 15), correlates with the progradation of the Anisian reef complex and the development of a zone of prolonged exposure and tepee development in the interior of the Great Bank of Guizhou (Figure 15). Sequences 6 and 7 and the drowning of the Great Bank of Guizhou (Figure 15, MAX F-8) postdate the CPP, but have been correlated with sequences and drowning of the Yangtze platform in the Guiyang and Zhenfeng areas (Koenig et al., 2001).

Basinwide correlation of depositional sequences in the Nanpanjiang Basin demonstrates significant control of eustatic sea level fluctuations on platform evolution, although the overall architecture, basin-margin geometries, and timing of drowning were primarily influenced by patterns of tectonic subsidence and timing of siliciclastic basin fill as discussed above.

IMPLICATIONS FOR TECTONICS OF THE NANPANJIANG BASIN

Interpretation of the tectonic history of the Nanpanjiang Basin is complicated because the nature of the southern boundary of the South China block remains controversial, in part because the bordering Songma-Ailaoshan zone has been intensely deformed by Cretaceous–Tertiary shear (Tapponier et al., 1990; Lepvrier et al., 1997). Critical unresolved issues include where a thrust belt may lie, whether the Songma represents an Indosinian suture, and whether the Nanpanjiang Basin lies on an overriding or underriding plate.

The subsidence patterns and the regional depositional history suggest Triassic foreland development in the Nanpanjiang Basin. The width of the Nanpanjiang Basin, approximately 500 km (310 mi) from north to south, is, however, quite large in comparison with other foreland basins (cf., Beaumont, 1981; Allen et al., 1986; DeCelles and Giles, 1996). Two possibilities may account for the great width of the basin: (1) Subsidence was generated primarily by dynamic topography resulting from mantle density variations and viscous flow in the mantle along the subducting slab (Gurnis, 1992, 1993); or (2) subsidence resulted from peripheral foreland evolution in which the subduction load of the downgoing lithosphere resulted in widespread foredeep subsidence (DeCelles and Giles, 1996). In the former case, the Nanpanjiang Basin would have developed as a retroarc basin of a Songma suture zone to the south (Figure 2); the thick volcanic pile in the Chongzuo area would represent an arc developed approximately 150 km (93 mi) north of the subduction zone. If the latter case of a peripheral foreland-basin model were correct, then the southward-thickening volcanic package would have been derived from an arc developed on the overriding plate converging from the south. However, the problem of identifying thrust sheets responsible for foreland-basin loading remains.

Another difficulty with invoking foreland-basin evolution is that a zone of uplift and unconformity development, consistent with a migrating forebulge expected from models (cf. Beaumont, 1981) has not been identified. DeCelles and Giles (1996) pointed out that forebulges have been difficult to identify, and that in marine foreland basins, carbonate platforms may nucleate on the forebulge (cf. Dorobek, 1995; Giles and Dickinson, 1995). Giles (2006, personal communication) suggested that a significant forebulge may not develop if subsidence is generated primarily by dynamic topography. Alternatively, Triassic carbonate platforms in the Nanpanjiang Basin may have nucleated on a subtle forebulge then aggraded vertically and progressively drowned as the foredeep and forebulge migrated northward.

Thermochronology data indicate widespread high-temperature metamorphism across northern Vietnam during the Early and Middle Triassic (Carter et al., 2001). The metamorphism was interpreted as a result of convergent tectonism during the Indosinian orogeny (Carter et al., 2001). However, following Metcalfe (1996), they interpreted the Indochina and South China blocks to have been joined prior to the Triassic. On that basis, they concluded that the metamorphic event resulted from collision with the Siamo-Sibumasu block along the western margin of Indochina. The thermochronology could equally support the metamorphism associated with convergence of the Indochina and South China blocks. Lepvrier et al. (1997), using structural data and ^{40}Ar-^{39}Ar dates, came to the similar conclusion that northern Indochina (northern Vietnam, Laos, and northern Thailand) experienced Triassic dextral shear resulting from the oblique convergence of the Indochina block with the South China plate. The situation becomes significantly more complex if Indosinian tectonism resulted from the nearly simultaneous collision of several continental blocks.

An extensive Cretaceous–Tertiary tectonic overprint, primarily left-lateral shear with offsets of hundreds of kilometers associated with Himalayan tectonics, makes it exceedingly difficult to interpret the timing and position of suture zones within the blocks bordering south China (cf. Tapponier et al., 1990). Thus, the subsidence and sedimentation history of the Nanpanjiang Basin inboard of these zones provide valuable insight into the tectonics of the region not possible from the deformation zones themselves. Plate boundaries are commonly so complex and overprinted that it is nearly impossible to deduce the tectonic history from these areas. The fingerprints left in the sedimentary basins, however, permit the evaluation of different tectonic scenarios. The subsidence patterns, basin-fill history, and distribution of volcanics are most consistent with Triassic convergence along the southern margin of the South China plate.

IMPLICATIONS FOR HYDROCARBON EXPLORATION

This study provides outcrop analogs and evolution models for the exploration of large, isolated carbonate platforms, especially those developed in foreland basins. The platforms of the Nanpanjiang Basin can be considered giant isolated platforms (2000–18,000 km^2; 772–6949 mi^2) that rival or exceed the area of large productive platforms, such as the Horseshoe Atoll (Pennsylvanian, 14,000 km^2 [5405 mi^2]); Golden Lane (Cretaceous, 8000 km^2 [3088 mi^2]), Natuna (Miocene, Segitiga platform, 1400 km^2 [540 mi^2]), and Tengiz (Carboniferous, 580 km^2 [223 mi^2]) (Wilson, 1975; Switzer et al., 1994; Bachtel et al., 2000; Weber et al., 2003).

Although the Nanpanjiang Basin itself has poor hydrocarbon potential resulting from deep burial and overmaturation of source rocks (Halley et al., 1988), the Lower Triassic strata provide facies models with potential reservoirs and source rocks (Sun et al., 1989) useful for continued exploration in coeval strata in the gas-producing Sichuan Basin.

CONCLUSIONS

1. Tectonic subsidence was a dominant factor in the evolution of isolated carbonate platforms within the Nanpanjiang Basin. Platforms in the southern part of the basin responded to higher rates of subsidence and earlier onset of peak subsidence by developing great thickness, margin backstep, pinnacles, and eventual drowning. Southerly platforms were terminated by drowning and buried by siliciclastics earlier than the Great Bank of Guizhou and the attached Yangtze platform in the northern part of the basin. Timing of siliciclastic basin-fill dictated differences in platform-margin geometry, e.g., in slope angle, relief above basin floor, and platform progradation. Eustatic sea level fluctuations imparted a basinwide sequence-stratigraphic signal.
2. The CPP evolved from a low-relief bank with oolite shoals in the Early Triassic, through backstepping and drowning early in the Middle Triassic (Bithynian), to develop small pinnacle platforms with *Tubiphytes* reefs (Bithynian and Pelsonian). The pinnacle platforms drowned and were buried by siliciclastics in the Middle Triassic (Pelsonian).
3. The evolution of the Heshan and Debao platforms paralleled that of the CPP, except that the Heshan platform drowned and was completely buried by siliciclastics slightly earlier (Middle Triassic, Aegean), whereas the Debao platform developed Middle Triassic pinnacles.
4. The Great Bank of Guizhou has a longer history, but substantially thinner strata, than the southerly platforms. It evolved as a megabank with a ramp profile in the Early Triassic and progressively steepened and increased in relief from a reef-rimmed to an escarpment profile in the Middle Triassic. The platform drowned and was buried by siliciclastics in the Late Triassic (Carnian).
5. Patterns and rates of subsidence are consistent with foreland-basin development, presumably resulting from convergence of the South China and Indochina plates. Accelerating subsidence in the Early and Middle Triassic is consistent with foreland-basin patterns and rates. Greater subsidence and earlier peak-subsidence rates in the southern part of the basin than in the north point to convergence and tectonic loading from the south. The correlation of platform evolution with patterns of subsidence indicates tectonic control on overall platform architecture and history. Correspondence of platform termination and siliciclastic burial to peak subsidence rates is consistent with platform termination by drowning.
6. Early Middle Triassic (Aegean) volcanism interrupted carbonate-platform growth proximal to the volcanic source area in the southernmost part of the basin (Chongzuo area), although it had no significant impact on the evolution of platforms in the central and northern parts of the basin.
7. Earlier arrival of siliciclastic turbidites in the southern basin than in the north is consistent with a southerly source area. Siliciclastic influx impacted carbonate-platform evolution through modifying the geometry of the basin margin. Early arrival of clastics in the Pingguo area resulted in the aggradation of

pinnacle platforms concurrent with siliciclastic basin fill, producing lower slope angles, reduced syndepositional relief, intertonguing of basin-margin carbonates and siliciclastics, and ultimately, a late stage of platform progradation over basin-filling siliciclastics. In contrast, later arrival of siliciclastic turbidites in the northern basin caused the Great Bank of Guizhou to develop a progressively steepening profile and a high-relief escarpment as subsidence and increasing water depths locked the platform into aggradation.

8. Basinwide correlation of depositional sequences using biostratigraphy, lithostratigraphy, and magnetic susceptibility demonstrates that eustasy was important in platform evolution, despite the predominant function of tectonic subsidence in overall platform architecture. Comparison of subsidence histories indicates that platform drowning was primarily controlled by subsidence. This drowning marked the end of carbonate-platform sedimentation in the Nanpanjiang Basin.

REFERENCES CITED

Allen, P. A., P. Homewood, and G. D. Williams, 1986, Foreland basins, an introduction, *in* P. A. Allen and P. Homewood, eds., Foreland basins: International Association of Sedimentologists Special Publication 8, p. 3–12.

Al-Tawil, A., T. C. Wynn, and J. F. Read, 2003, Sequence response of a distal-to-proximal foreland ramp to glacio-eustacy and tectonics; Mississippian, Appalachian Basin, West Virginia–Virginia, U.S.A., *in* W. M. Ahr, P. M. Harris, W. A. Morgan, and I. D. Somerville, eds., Permo-Carboniferous carbonate platforms and reefs: SEPM Special Publication 78, p. 11–34.

Bachtel, S. L., R. Kissling, D. Martono, S. Rahardjanto, P. Dunn, and B. Macdonald, 2000, Structural influence on carbonate platform architecture; origin, growth, and demise of the Miocene–Pliocene Segitiga Platform, East Natuna Sea, Indonesia (abs.): AAPG Annual Meeting Program, v. 9, p. A8.

Beaumont, C., 1981, Foreland basins: Geophysical Journal of the Royal Astronomical Society, v. 65, p. 291–329.

Bond, G. C., and M. A. Kominz, 1984, Construction of tectonic subsidence curves for the Early Paleozoic miogeosyncline, southern Canadian Rocky Mountains: Implications for subsidence mechanisms, age of breakup and crustal thinning: Geological Society of America Bulletin, v. 95, p. 155–173.

Carter, A., D. Roques, C. Bristow, and P. Kinny, 2001, Understanding Mesozoic accretion in southeast Asia: Significance of Triassic thermotectonism (Indosinian orogeny) in Vietnam: Geology, v. 29, p. 211–214.

Chaikin, D. H., 2004, Sedimentology and provenance of the Bianyang Formation, Guizhou Province, south China: Master's thesis, University of Kansas, Lawrence, Kansas, 320 p.

Chen, J., K. A. Foland, F. Xing, X. Xu, and T. Zhou, 1991, Magmatism along the southeast margin of the Yangtze block: Precambrian collision of the Yangtze and Cathasia blocks of China: Geology, v. 19, p. 815–818.

Chung, S. L., and B. M. Jahn, 1995, Plume-lithosphere interaction in generation of Emeishan flood basalts at the Permian–Triassic boundary: Geology, v. 23, p. 889–892.

Crick, R. E., B. B. Ellwood, A. El Hassani, R. Feist, and J. Hladil, 1997, Magnetosusceptibility event and cyclostratigraphy (MSEC) of the Eifelian–Givetian GSSP and associated boundary sequences in North Africa and Europe: Episodes, v. 20, p. 167–175.

DeCelles, P. G., and K. A. Giles, 1996, Foreland basin systems: Basin Research, v. 8, p. 105–123.

Dorobek, S. L., 1995, Synorogenic carbonate platforms and reefs in foreland basins: Controls on stratigraphic evolution and platform/reef morphology, *in* S. L. Dorobek and G. M. Ross, eds., Stratigraphic evolution of foreland basins: SEPM Special Publication 52, p. 127–147.

Dorobek, S. L., S. K. Reid, M. Elrick, G. C. Bond, and M. A. Kominz, 1991, Subsidence across the Antler foreland of Montana and Idaho: Tectonic versus eustatic effects, *in* E. K. Franseen, W. L. Watney, C. G. St. C. Kendall, and W. Ross, Sedimentary modeling: Computer simulations and methods for improved parameter definition: Kansas Geological Survey Bulletin, v. 233, p. 231–252.

Eberli, G. P., and R. H. Ginsburg, 1987, Segmentation and coalescence of platforms, Tertiary, NW Great Bahama Bank: Geology, v. 15, p. 75–79.

Ellwood, B. B., R. E. Crick, and A. El Hassani, 1999, The magnetosusceptibility event and cyclostratigraphy (MSEC) method used in geological correlation of Devonian rocks from Anti-Atlas Morocco: AAPG Bulletin, v. 83, p. 1119–1134.

Enkin, R. J., Yang Zhenyu, Chen Yan, and V. Courtillot, 1992, Paleomagnetic constraints on the geodynamic history of the major blocks of China from the Permian to the present: Journal of Geophysical Research, v. 97, no. B10, p. 13,953–13,989.

Enos, P., 1995, Permian of China, *in* P. A. Scholle, T. M. Peryt, and D. S. Ulmer-Scholle, eds., The Permian of northern Pangea: Berlin, Springer-Verlag, v. 2, p. 225–256.

Enos, P., and R. D. Perkins, 1977, Quaternary sedimentation in south Florida: Geological Society of America Memoir 147, 198 p.

Enos, P., Wei Jiayong, and Yan Yangji, 1997, Facies distribution and retreat of Middle Triassic platform margin, Guizhou Province, south China: Sedimentology, v. 44, no. 3, p. 563–584.

Enos, P., Wei Jiayong, and D. J. Lehrmann, 1998, Death in Guizhou—Late Triassic drowning of the Yangtze carbonate platform: Sedimentary Geology, v. 118, p. 55–76.

Enos, P., D. J. Lehrmann, Wei Jiayong, Yu Youyi, Xiao Jiafei, D. H. Chaikin, M. Minzoni, A. K. Berry, and P. Montgomery, in press, Triassic evolution of the Yangtze platform in Guizhou Province, P.R.C.: Geological Society of America Special Paper 417.

Fan, C., and Y. Zhang, 1994, The structure and tectonics of western Yunnan: Journal of Southeast Asian Earth Sciences, v. 9, p. 355–361.

Findlay, R. H., and P. T. Trinh, 1997, The structural setting of the Song Ma region, Vietnam and the Indochina–South China plate boundary problem: Gondwana Research, v. 1, p. 11–33.

Gilder, S. A., R. S. Coe, Wu Haoruo, Kuang Guodun, Zhao Xixi, and Wu Qi, 1995, Triassic paleomagnetic data from south China and their bearing on the tectonic evolution of the western circum-Pacific region: Earth and Planetary Science Letters, v. 131, p. 269–287.

Giles, K. A., and W. R. Dickinson, 1995, The interplay of eustacy and lithospheric flexure in forming stratigraphic sequences in foreland settings: An example from the Antler foreland, Nevada and Utah, *in* S. L. Dorobek and G. M. Ross, eds., Stratigraphic evolution of foreland basins: SEPM Special Publication 52, p. 187–211.

Goldhammer, R. K., P. J. Lehmann, and P. A. Dunn, 1993, The origin of high-frequency platform carbonate cycles and third-order sequences (Lower Ordovician El Paso Group, west Texas): Constraints from outcrop data and stratigraphic modeling: Journal of Sedimentary Petrology, v. 63, p. 318–359.

Greenlee, S. M., and P. J. Lehmann, 1993, Stratigraphic framework of productive carbonate buildups, *in* R. G. Loucks and J. F. Sarg, eds., Carbonate sequence stratigraphy: AAPG Memoir 57, p. 43–62.

Guangxi Bureau of Geology and Mineral Resources, 1985, Regional geology of Guangxi (in Chinese, with English summary): Geological Memoir 1, no. 3, 785 p., scale 1:1,000,000.

Guangxi Bureau of Geology and Mineral Resources, 2000, Regional geological map of Guangxi (in Chinese, with English summary): scale 1:500,000, 4 sheets.

Guizhou Bureau of Geology and Mineral Resources, 1987, Regional geology of Guizhou Province (in Chinese, with English summary): Geological Memoir 1, no. 6, 700 p., scale 1:500,000.

Gupta, S., 1989, Mesozoic overthrust tectonics in south China; discussion: Geology, v. 16, p. 418.

Gurnis, M., 1992, Rapid continental subsidence following the initiation and evolution of subduction: Science, v. 255, p. 1556–1558.

Gurnis, M., 1993, Depressed continental hypsometry behind oceanic trenches: A clue to subduction control on sea-level changes: Geology, v. 21, p. 29–32.

Halley, R. B., J. T. Parrish, Xie Zhan, Hu Wenhai, P. A. Scolle, Su Zhongrui, Zhang Yirong, Huang Yunming, and Li Guangkuan, 1988, Thermal and cementation histories of Permian shelf-edge carbonate rocks in the Nanpanjiang Basin, south China, *in* H. C. Wagner, L. C. Wagner, F. F. Wang, and F. L. Wong, eds., Petroleum resources of China and related subjects: Circum-Pacific Council for Energy and Mineral Resources, Earth Science Series, v. 10, p. 627–635.

Hallock, P., and W. Schlager, 1986, Nutrient excess and the demise of coral reefs and carbonate platforms: Palaios, v. 1, p. 1156–1166.

He, Ziai, 1986, Formation environment of turbidity current deposits in the Middle Triassic of Guizhou and Guangxi: Oil and Gas Geology, v. 7, no. 3, p. 207–217.

Hou, Fanghao, and Huang Jixiang, 1984, Research into the Permian and Triassic volcaniclastic turbidites of the Nanpan River sag: Acta Sedimentologica Sinica, v. 3, p. 256–264.

Hsü, K. J., Sun Shu, Li Jiliang, Chen Haihong, Pen Haipo, and A. M. C. Sengör, 1988, Mesozoic overthrust tectonics in south China: Geology, v. 16, p. 418–421.

Huang, Jiqing, 1978, An outline of the tectonic characteristics of China: Ecologae Geologicae Helvetiae, v. 71, p. 611–635.

Huang, Jiqing, and Chen Bingwei, 1987, The evolution of the Tethys in China and adjacent regions: Beijing, Geological Publishing House, 109 p.

Hutchinson, C. S., 1989, The palaeo-Tethyan realm and Indosinian orogenic system of southeast Asia, *in* A. M. C. Sengör, ed., Tectonic evolution of the Tethyan region: NATO ASI Series, Series C: Mathematical and Physical Sciences, v. 259, p. 585–643.

Ingersoll, R. V., W. R. Dickinson, and S. A. Graham, 2002, Remnant-ocean submarine fans; largest sedimentary systems on Earth, *in* M. A. Chan and A. A. Archer, eds., Extreme depositional environments; mega end members in geologic time: Geological Society of America Special Paper 370, p. 191–208.

James, N. P., 1997, The cool-water carbonate depositional realm, *in* N. P. James and J. A. D. Clarke, eds., Cool-water carbonates: SEPM Special Publication 56, p. 1–20.

Kessel, B. J., J. D. Gross, and D. J. Lehrmann, 2002, Facies and microfossil study of the mechanisms and timing of termination of the Heshan carbonate platform, Nanpanjiang Basin, south China (abs.): Geological Society of America Abstracts with Programs, v. 34, no. 6, p. 15.

Klimetz, M. P., 1983, An outline of the Mesozoic plate evolution of eastern China: Tectonics, v. 2, p. 139–166.

Koenig, J., P. Dillett, D. Lehrmann, and P. Enos, 2001, Structural and paleogeographic elements of the Nanpanjiang Basin, Guizhou, Guangxi, and Yunnan provinces, south China: A compilation from satellite images, regional geologic maps and ground observations (abs.): AAPG Annual Meeting Program, v. 10, p. A107.

Lacassin R., P. H. Leloup, P. T. Trinh, and P. Tapponier, 1998, Unconformity of red sandstones in North Vietnam: Field evidence for Indosinian orogeny in northern Indochina?: Terra Nova, v. 10, p. 106–111.

Lehrmann, D. J., Wei Jiayong, and P. Enos, 1998, Controls on facies architecture of a large Triassic carbonate platform: The Great Bank of Guizhou, Nanpanjiang Basin, south China: Journal of Sedimentary Research, v. 68, p. 311–326.

Lehrmann, D. J., Yang Wan, Wei Jiayong, Yu Youyi, and Xiao Jiafei, 2001, Lower Triassic peritidal cyclic limestone: An example of anachronistic carbonate facies from the Great Bank of Guizhou, Nanpanjiang Basin, Guizhou Province, south China: Palaeogeography, Palaeoclimatology, Palaeoecology, v. 173, no. 3–4, p. 103–123.

Lehrmann, D. J., J. L. Payne, S. V. Felix, P. M. Dillett, Wang Hongmei, Yu Youyi, and Wei Jiayong, 2003, Permian–Triassic boundary sections from shallow-marine carbonate platforms of the Nanpanjiang Basin, south China: Implications for oceanic conditions associated with the end-Permian extinction and its aftermath: Palaios, v. 18, p. 138–152.

Lehrmann, D. J., J. Ramezani, S. A. Bowring, M. W. Martin, P. Montgomery, P. Enos, J. L. Payne, M. J. Orchard, Wang Hongmei, and Wei Jiayong, 2006, Timing of recovery from the end-Permian extinction: Geochronologic and biostratigraphic constraints from south China: Geology, v. 34, p. 1053–1056.

Lepvrier, C., H. Maluski, N. Van Vuong, D. Roques, V. Axente, and C. Rangin, 1997, Indosinian NW-trending shear zones within the Truong Son belt (Vietnam) ^{40}Ar-^{39}Ar Triassic ages and Cretaceous to Cenozoic overprints: Tectonophysics, v. 283, p. 105–127.

Lin, Jinlu, M. Fuller, and Zhang Wenyou, 1985, Preliminary Phanerozoic polar wander paths from the North and South China blocks: Nature, v. 313, p. 444–449.

Liu, Baojun, and Xu Xiaosong, eds., 1994, Atlas of lithofacies and paleogeography of south China: Beijing, Science Press, 192 p.

Loucks, R. G., and J. F. Sarg, eds., 1993, Carbonate sequence stratigraphy: AAPG Memoir 57, 545 p.

Luo, Zhili, Jin Yinzhong, and Zhao Xikui, 1990, Emei taphrogenesis of the upper Yangtze platform in south China: Geological Magazine, v. 5, p. 393–405.

Meng, Qingren, and Zhang Guowei, 1999, Timing of collision of the North and South China blocks: Controversy and reconciliation: Geology, v. 27, p. 123–126.

Metcalfe, I., 1996, Pre-Cretaceous evolution of SE Asian terrranes, *in* R. Hall and D. Blundell, eds., Tectonic evolution of southeast Asia: Geological Society (London) Special Publication 106, p. 91–122.

Metcalfe, I., 2002, Permian tectonic framework and palaeogeography of SE Asia: Journal of Asian Earth Sciences, v. 20, no. 6, p. 551–566.

Newkirk, T. T., D. Lehrmann, and G. Hudak, 2002, Tephrastratigraphy and analysis of tectonic setting of Triassic intermediate volcanic strata: Nanpanjiang Basin, south China (abs.): Geological Society of America Abstracts with Programs, v. 34, no. 6, p. 512.

Ogg, J. G., 2004, The Triassic period, *in* F. M. Gradstein, J. G. Ogg, and A. G. Smith, eds., A geologic time scale 2004: Cambridge, United Kingdom, Cambridge University Press, 589 p.

Proust, J. N., B. I. Chuvashov, E. Vennin, and T. Boisseau, 1998,

Carbonate platform drowning in a foreland setting: The mid-Carboniferous platform in the western Urals (Russia): Journal of Sedimentary Research, v. 68, no. 6, p. 1175–1188.
Qing, Jianhua, Wu Yinglin, Yan Yangji, and Zhu Zhongfa, 1991, Hercinian–Indosinian geotectonic evolution of Dian-Qian-Gui Basin, southwestern China-north marginal basin of the eastern end of east Tethys: International Symposium on Gondwana Dispersion and Asian Accretion: International Geological Correlation Programme Project 321, p. 206–211.
Ren, Jishun, Jiang Chunfa, Zhang Zhengkun, and Qin Deyu, 1987, Geotectonic evolution of China: Beijing, Science Press, 203 p.
Rodgers, J., 1989, Comment on ''Mesozoic overthrust tectonics in south China'': Geology, v. 17, p. 671–672.
Rowley, D. B., A. M. Ziegler, and Nie Gyou, 1989, Comment on ''Mesozoic overthrust tectonics in south China'': Geology, v. 17, p. 384–386.
Saller, A., R. Armin, L. O. Ichran, and C. Glenn-Sullivan, 1993, Sequence stratigraphy of aggrading and backstepping carbonate shelves, Oligocene, central Kalimantan, Indonesia, *in* R. G. Loucks and J. F. Sarg, eds., Carbonate sequence stratigraphy: AAPG Memoir 57, p. 267–290.
Schlager, W., 1999, Scaling of sedimentation rates and drowning of reefs and carbonate platforms: Geology, v. 27, no. 2, p. 183–186.
Schlager, W., D. Marsal, P. A. Van der Geest, and A. Sprenger, 1998, Sedimentation rates, observation spans, and the problem of spurious correlation: Mathematical Geology, v. 30, p. 547–556.
Sengör, A. M. C., 1987, Tectonics of the Tethysides-Orogenic collage development in a collisional setting: Annual Review of Earth and Planetary Sciences, v. 15, p. 213–244.
Smith, L. B., and J. F. Read, 2001, Discrimination of local and global effects on upper Mississippian stratigraphy, Illinois Basin, U.S.A: Journal of Sedimentary Research, v. 71, no. 6, p. 985–1002.
Song, Xieyan, Zhou Meifu, Cao Zhimin, and P. T. Robinson, 2004, Late Permian rifting of the South China craton caused by the Emeishan mantle plume?: Journal of the Geological Society (London), v. 161, p. 773–781.
Sun, Shu, Li Jilang, Chen Haihong, Peng Haipo, K. J. Hsü, and J. W. Shelton, 1989, Mesozoic and Cenozoic sedimentary history of south China: AAPG Bulletin, v. 73, no. 10, p. 1247–1269.
Switzer, S. B., W. G. Holland, D. S. Christie, G. C. Graf, A. S. Hedinger, and R. J. McAuley, 1994, Devonian Woodbend-Winterburn strata of the Western Canada sedimentary basin, *in* G. D. Mossop and I. Shetsen, compilers, Geological atlas of the Western Canada sedimentary basin: American Geological Institute, p. 164–202.
Tan, Xiaodong, K. P. Kodama, Wang Pengyan, and Fang Dajun, 2000, Paleomagnetism of Early Triassic limestones from the Huanan block, south China: No evidence for separation between the Huanan and Yangtze blocks during the early Mesozoic: Geophysical Journal International, v. 142, no. 1, p. 241–256.
Tapponier, P., R. Lacassin, P. H. Leloup, U. Scharer, D. Zhong, H. Wu, X. Liu, S. Ji, L. Zhang, and J. Zhou 1990, the Ailao Shan/Red River metamorphic belt: Tertiary left-lateral shear between Indochina and south China: Nature, v. 343, p. 431–437.
Van der Voo, R., 1993, Paleomagnetism of the Atlantic, Tethys and Iapetus oceans: Cambridge, United Kingdom, Cambridge University Press, 411 p.
Wang, Hongzhen, ed., 1985, Atlas of the paleogeography of China: Beijing, Cartographic Publishing House, 281 p.
Weber, J. L., B. P. Francis, P. M. Harris, and M. Clark, 2003, Stratigraphy, facies, and reservoir distribution, Tengiz field, Kazakhstan, *in* W. M. Ahr, P. M. Harris, W. A. Morgan, and I. D. Somerville, eds., Permo-Carboniferous carbonate platforms and reefs: SEPM Special Publication 78, p. 351–394.
Wilson, J. L., 1975, Carbonate facies in geologic history: New York, Springer-Verlag, 471 p.
Wu, Jiang, and Li Sitang, 1993, Sedimentology of the Middle Triassic gold-bearing turbidite series in the northwestern Guangxi Zhuang autonomous region, China: Geoscience, v. 7, no. 2, p. 127–136.
Xia, Bangdong, Fang Zhong, Lu Hongbo, Zhu Bin, Zhou Weiming, and Yang Huiming, 1993, The Middle Triassic back-arc flysch in Nanpanjiang area, southwest China: Journal of Nanjing University, v. 5, no. 3, p. 320–329.
Xu, Xiaoxong, Xu Qiang, Pan Guiting, and Liu Qiaohong, 1996, Palaeogeography of the south China continent and its correlation with Pangea: Sedimentary Facies and Palaeogeography, v. 16, no. 2, p. 1–23.
Yunnan Bureau of Geology and Mineral Resources, 1984, Regional geology of Yunnan Province: Geological Memoires 1, no. 6, 700 p., scale 1:500,000.
Zhang, Hongfei, Gao Shan, Zhang Benren, Luo Tingchuan, and Yin Wenli, 1997, Pb isotopes of granitoids suggest Devonian accretion of the Yangtze (south China) craton to North China craton: Geology, v. 25, p. 1015–1018.
Zhang, Jiyan, 1986, Middle Triassic gravity-flow deposits in western Guangxi: Regional Geology of China, v. 2, p. 125–132.
Zhang, Zhimeng, J. G. Liou, and R. G. Coleman, 1984, An outline of the plate tectonics of China: Geological Society of America Bulletin, v. 95, p. 295–312.
Zhang, Zuqi, 1984, The Permian system in south China: Newsletters on Stratigraphy, v. 13, p. 156–174.